Discovery of a Potent HDAC3/6 Selective Dual Inhibitor

Uttara Soumyanarayanan,[1] Pondy Murugappan Ramanujulu,[1,2] Nurulhuda Mustafa,[3] Shozeb Haider,[4] Adina Huey Fang Nee,[5] Jie Xin Tong,[6] Kevin SW Tan,[6] Wee Joo Chng,[3,5,7] Brian W Dymock[1,*]

[1] Department of Pharmacy, National University of Singapore, 18 Science Drive 4, Singapore 117543

[2] Life Sciences Institute, Centre for Life Sciences Level 5, 28 Medical Drive, National University of Singapore, Singapore 117456

[3] Department of Medicine, Yong Loo Lin School of Medicine, National University of Singapore, 1E Kent Ridge Road, NUHS Tower Block Level 10, Singapore 119228

[4] UCL School of Pharmacy, 29-39 Brunswick Square, Bloomsbury, London WC1N 1AX, UK

[5] Cancer Science Institute, Singapore, National University of Singapore

[6] Department of Microbiology and Immunology, Yong Loo Lin School of Medicine, 5 Science Drive 2, Singapore 117545

[7] National University Cancer Institute of Singapore, National University Health System

[*] **Corresponding author contact:**

Email address: bwdnus@gmail.com

Current Address: UniQuest Pty Ltd, Level 7, General Purpose South Building (Building 78), Staff House Road, The University of Queensland, Brisbane, Queensland 4072, Australia

Abstract

Herein, we report the discovery of a dual histone deacetylase inhibitor displaying a unique HDAC3/6 selectivity profile. An initial strategy to merge two epigenetic pharmacophores resulted in the discovery of potent HDAC6 inhibitors with selectivity over HDAC1. Screening in an HDAC panel revealed only HDAC3 as an additional low nanomolar activity. Low micromolar antiproliferative activities against two breast cancer and four hematological cancer cell lines was supported by pharmacodynamic studies on a preferred molecule, **25d**, supporting the HDAC inhibitory profile in cells. Apoptosis was identified as one of the main cell death pathways. Modelling studies of **25d** against HDAC1,2,3 and 6 further provided insights on the orientation of specific residues relevant to compound potency explaining the observed HDAC3/6 selectivity. A subset of the compounds also exhibited good antimalarial activities particularly against the chloroquine-resistant strain K1 of *P.falciparum*. *In vitro* studies revealed a favourable DMPK profile warranting further investigation of the therapeutic potential of these compounds.

Introduction

Targeted therapies have revolutionised the treatment of cancers over the last two decades and are the cornerstone of personalised medicine. Drug development today heavily relies on detailed knowledge of protein targets or genes that are specifically dysregulated in pathological conditions.[1,2] Epigenetics is one such rapidly evolving field offering a plethora of opportunities for developing targeted therapies for cancer, cardiovascular and neurological disorders as well as for infectious diseases like malaria.[3,4]

Epigenetics involves post-translational modifications (PMTs) which activate or repress specific gene functions, consequently altering cellular phenotypes, without change in the nucleic acid sequence.[5] PTMs, also known as epigenetic marks, not only occur on DNA but also on histone proteins, eventually leading to chromatin remodelling and altered gene expression. These modifications, either silencing tumour suppressor genes or activating cancer-survival pathways, are critical epigenetic carcinogenesis mechanisms. DNA is primarily methylated whereas histones undergo a greater variety of PTMs such as methylation, acetylation, phosphorylation, sumoylation and glycosylation. Epigenetic proteins are classified as writers, erasers or readers depending on their ability to create, erase or read epigenetic marks respectively.[6]

EHMT2 (G9a), a histone methyltransferase, is an epigenetic writer that catalyses mono- and di-methylation of lysine residues on histones, specifically H3K9Me1 and H3K9Me2. G9a upregulation, correlated with higher methylation levels, is associated with a variety of cancers including lung, prostate, and leukemias. Inhibition of G9a enzymatic activity in these cases has been demonstrated to inhibit cancer cell proliferation via various mechanisms including apoptosis and autophagy.[7,8] BIX01294 (**1**) and UNC0638 (**2**) (**Figure 1A**) were the earliest small molecule G9a inhibitors reported having biochemical potencies in the nanomolar concentration range against G9a.[9] The pharmacodynamic efficacy of **2** in reducing H3K9Me2

has been established in both MCF-7 and MDA-MB-231 breast cancer cells; challenges encountered in translating these activities to *in vivo* models were also reported.[10,11] Subsequently, Curry et al. demonstrated dual inhibition of HMTs G9a/EZH2 resulted in increased efficacy against breast cancer cells as opposed to G9a or EZH2 inhibition alone.[12] These results provide promising avenues for the development of G9a inhibitors as mono as well as dual epigenetic anticancer agents.

On the other hand, histone deacetylases (HDACs) are epigenetic erasers having a repressive influence on transcription by causing chromatin compaction.[13] Classical HDACs comprise Class I, II and IV enzymes having a Zinc-dependant catalytic domain whereas Class III HDACs have a Zinc independent active site. Hydroxamates, aliphatic acids, cyclic peptides and benzamides are some common chemical classes of HDAC inhibitors. Vorinostat (SAHA, **3**), a pan-HDAC hydroxamate inhibitor, was the first US FDA approved HDACi for clinical use.[14] Compound **3** and other HDACi, used either as monotherapy or in combination, have shown potential and importantly good tolerance in patients with hematological and solid malignancies including breast, colon, ovarian and renal cancers. These HDACi act via multiple pathways causing autophagic cell death, cell cycle arrest, senescence or by activating intrinsic or extrinsic apoptotic pathways.

Epigenetic events like acetylation and methylation have established roles in complex malarial parasite life cycles.[4] Resistance to standard antimalarial therapies like chloroquine (CQ) is a pressing issue and demands new therapies, ideally having a lower potential for resistance. G9a inhibitors like **1** and HDACi like **3** exhibit nanomolar efficacies against *P.falciparum strains*.[4,15] Dual epigenetic target inhibition offers opportunities to extend their therapeutic activities in this domain as well.

Given the number of PTMs histones are subjected to, these marks do not exist in isolation but are representative of a complex interplay between different epigenetic events. For example, cyclic peptide HDACi romidepsin suppresses the expression of G9a and associated H3K9Me2 and H3K9Me3 levels in H719 human lung cancer cells.[16] Further to this, HDACi trichostatin A (TSA) has been demonstrated to block both deacetylation as well as methylation of H3K9 at the CYP7A1 promoter, one of the key genes involved in bile acid synthesis.[17] A combination of TSA and **1** has been found to significantly decrease H3K9Me2 levels leading to enhanced improvement in the development of porcine cloned embryos.[18] This evidence provides a strong rationale for targeting multiple pathways (for example, methylation and deacetylation) that can potentially result in similar downstream functions like cell death or inhibition of cell proliferation.

Multi-target therapies particularly hold relevance in complex diseases like cancer that involve several independent mutations or dysregulated pathways, eventually leading to phenotypic changes at the individual cell level (cell growth, motility, differentiation).[19] Several dual inhibitors involving epigenetic target combinations DNMT/HDAC, G9a/DNMT1, HDAC/RTK, HDAC/Topoisomerase, HDAC/Proteasome and JAK/HDAC have been reported to have enhanced antitumour efficacies in both solid tumours and haematological malignancies.[20–26] A number of clinical trials are investigating the potential of DNMT inhibitors and HDACi as combinations with either chemotherapy or targeted therapies in breast cancer patients.[27]

Recently, Zhang et al. reported a library of small molecules and demonstrated G9a (7-99 μM) and HDAC (5-27 μM) inhibition against breast and cervical cancer cells.[28] While these molecules have provided important leads to developing dual inhibitors, there is much scope for discovering molecules with enhanced enzyme inhibitory capacities as well as antiproliferative activities.

In our present work, we have employed a pharmacophore merging strategy to design new molecules that incorporate pharmacophoric elements potentially applicable for both G9a MT and HDAC inhibition. We initially explored the structure-activity relationships (SAR) against HDAC1 and 6 and studied how a range of structural variations affect their enzymatic and cellular activities against cancer and malaria. We describe surprising selectivity of the new compounds towards HDACs and hence report what we believe to be the first HDAC3/6 dual inhibitor.

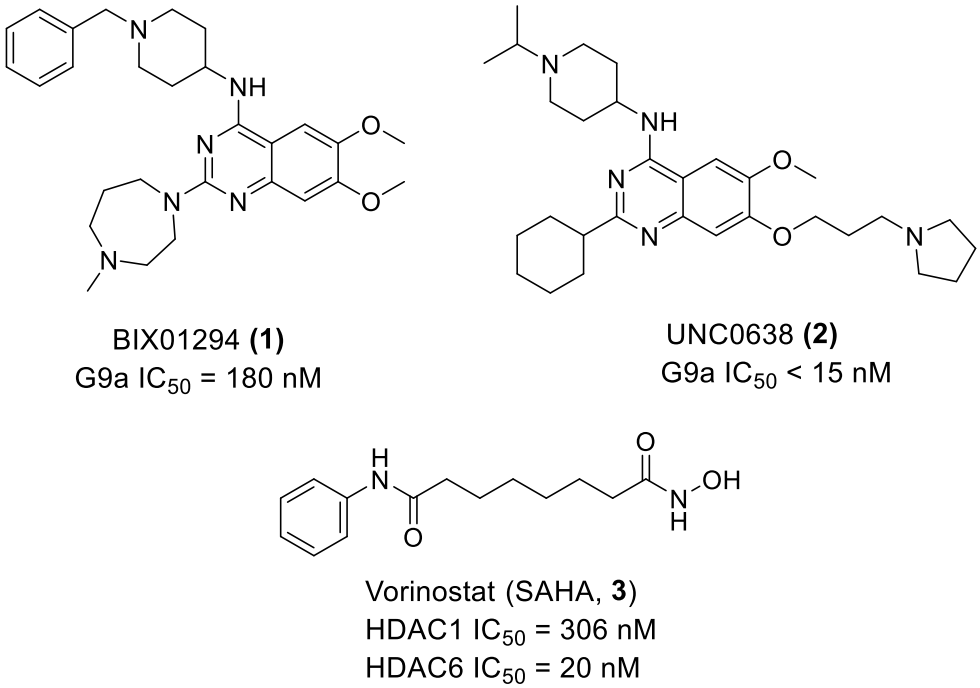

Figure 1. Structures of G9a inhibitors BIX01294 (**1**), UNC0638 (**2**) and HDACi vorinostat (SAHA, **3**)[9,29]

Design strategy: Pharmacophore merging

Vorinostat (SAHA, **3**), the first FDA approved HDAC inhibitor (**Figure 1B)**, was selected owing to its low molecular weight, simple structure and demonstrated value in our hands in HDAC dual inhibitor designs.[22–24] An essential binding feature of **3** is the hydroxamic acid terminus that interacts strongly with the Zn^{2+} co-factor present at the base of the HDAC substrate binding cavity. Drawing on our previous work, we selected an aniline derivative of **1**,

to be merged with **3**. With a shared phenyl ring, aniline **4** complements **3** facilitating a 'merging' strategy to form **5** (**Figure 2**).

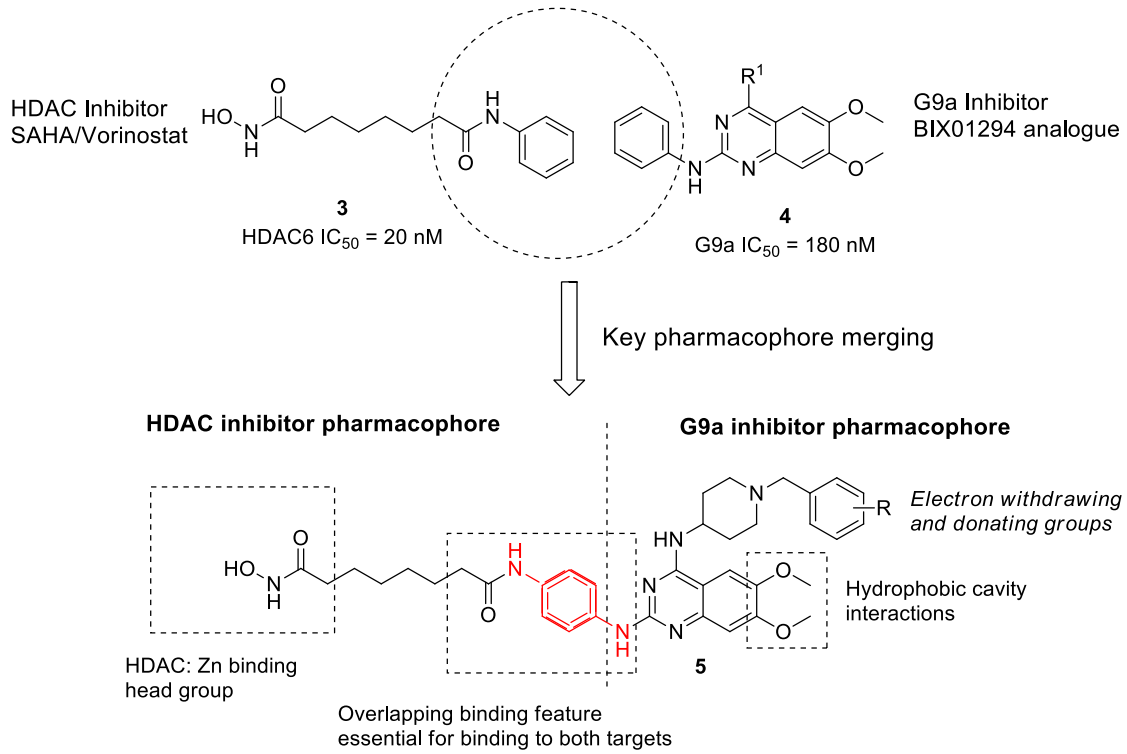

Figure 2. Pharmacophore merging leading to potential dual inhibitors

Preliminary docking studies of **5** (R=H) into the HDAC1 substrate pocket (**Figure 3A**) indicate the interactions made by the HDACi pharmacophore are similar to **3** with no apparent disruptive clashes from the proposed G9a inhibiting portion of the molecule.[30] Docking of **5** (R=H) into the peptide binding site of G9a (**Figure 3B**) strongly supported the ability of the binding pocket to accommodate the expected interactions of the G9ai pharmacophore; the docking showed no apparent clashes with the HDACi pharmacophore.

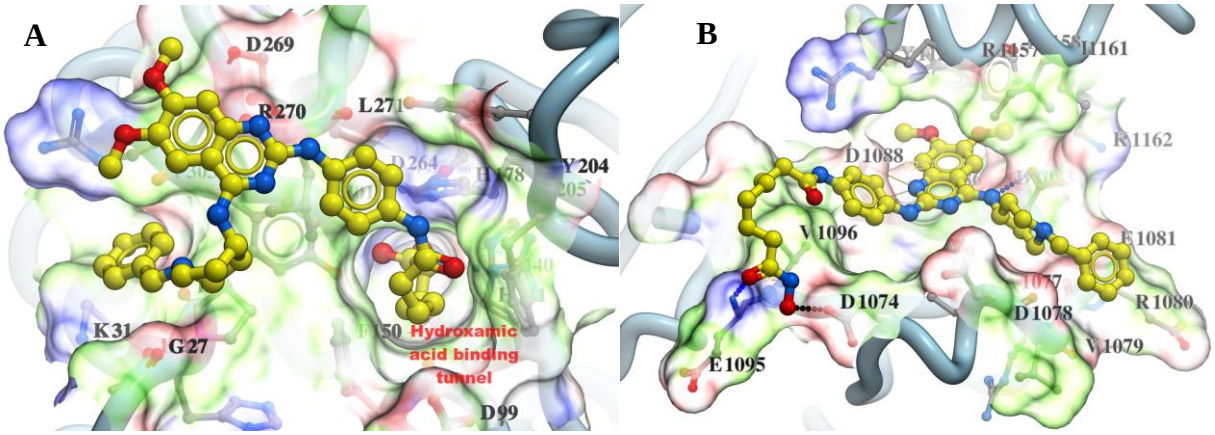

Figure 3. The binding site is illustrated as a surface representation. Hydrophobic residues in the receptor are coloured green, basic residue side chains are coloured blue and acidic residue side chains are coloured red. (A) Docking of **5** (R=H) into the HDAC1 (PDB id 4BKX) enzyme cavity shows the aliphatic chain binding to the hydroxamic acid binding tunnel is similar to 3; (B) Docking of **5** (R=H) into the G9a (PDB id 3RJW) enzyme cavity indicating potential hydrogen bonding interactions (E1095, D1074) of the HDAC binding component.

Having shown that the design of the prototype dual inhibitor **5** supports our hypothesis of epigenetic dual inhibitors binding to both targets G9a and HDAC, we developed a feasible synthetic route. We examined the effects of electron-donating and electron-withdrawing substituents on the phenyl ring at C-4 of the quinazoline. To expand the structural diversity of our investigations we incorporated a potential quinazoline-mimicking thienopyrimidine analogue in this series. We also investigated the significance of the aniline group at the C-2 position by replacing it with a saturated piperazine as well as by completely eliminating the aromatic ring altogether.

Chemistry

Both pharmacophoric precursors were synthesized individually and were coupled at a later stage to generate the dual inhibitor structure. For the synthesis of aniline precursor **9**, excess phenylenediamine (**6**) was mono Boc protected in cold DCM yielding **7,** following purification

to remove unreacted starting material and di-protected material.[31,32] Ethyl chloroformate (ECF) mediated amide coupling of **7** with suberic acid methyl ester to obtain **8** (**Scheme 1**).[33,34] Boc deprotection of **8**, carried out under acidic conditions (3 equiv. 98% H_2SO_4), afforded the first HDACi precursor **9** in good yield (77%). Piperazine derivative **12** was prepared similarly via an EDC-HOBt acid-amine coupling step followed by Boc-deprotection under acidic conditions.[35] Unlike **9** and **12**, the third precursor **21**, a straight chain amine, lacked aromatic or aliphatic rings at the position connecting C-2 of quinazoline and was obtained commercially.

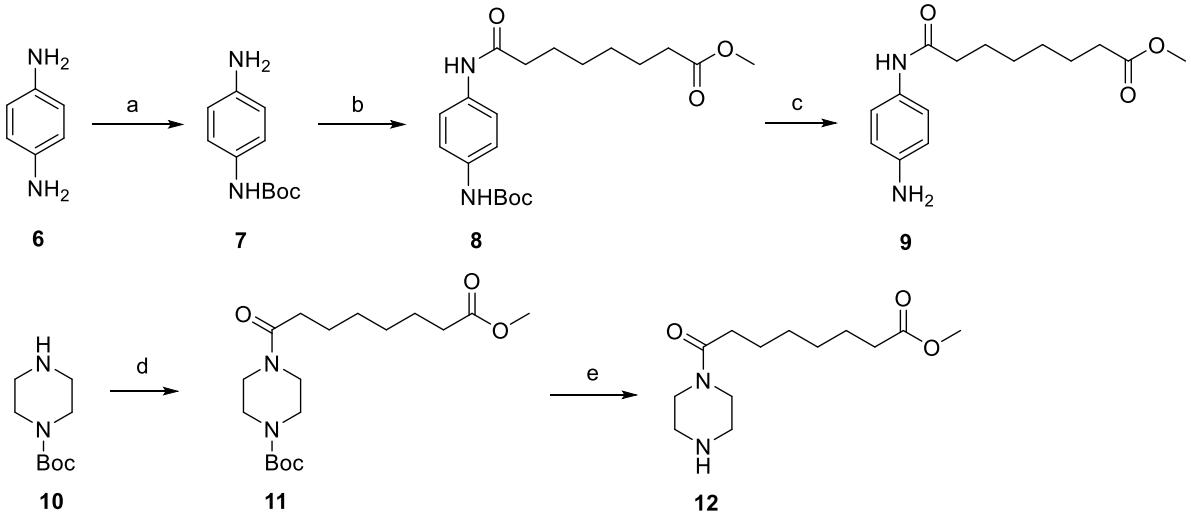

(a) $(Boc)_2O$, DCM, 0°C to RT, overnight, 65%; (b) Suberic acid monomethyl ester, $ClCO_2Et$, NMM, DCM, 0°C to RT, overnight, 84%; (c) 3 equiv. 98% H_2SO_4, EA, 4 h, RT, 77%.(d) Suberic acid monomethyl ester, EDC, HOBt, NMM, DCM, RT, overnight, 81%; (e) H_2SO_4, EA, RT, 4 h, 94%.

Scheme 1. Synthesis of HDAC inhibitor (HDACi) pharmacophore precursors

For the synthesis of G9a inhibitor precursor, 2,4-dichlorodimethoxy-quinazoline (**13**) was reacted directly with the respective benzyl substituted aminopiperidines to obtain derivatives **15a-c**. In cases where specific substitutions of 1-benzyl-4-aminopiperdine were commercially unavailable, we adopted an alternative route for synthesising the intermediates. Dichloroquinazoline **13** was subjected to nucleophilic displacement by Boc-protected aminopiperidine (**16**), and subsequently deprotected with acetyl chloride in methanol to yield free piperidine derivative **18** in good yield (**Scheme 2**).[36–38] Reductive amination of **18** with *p*-methoxy and *p*-fluoro derivatives of benzaldehyde provided compounds **15d,e**.[37] The [3,2-*d*]

isomer of 2,4-dichlorothienopyrimidine was reacted with 1-benzyl-4-aminopiperidine in DIPEA-mediated conditions at 50 °C to yield the 'scaffold-hopped' precursor **20**.

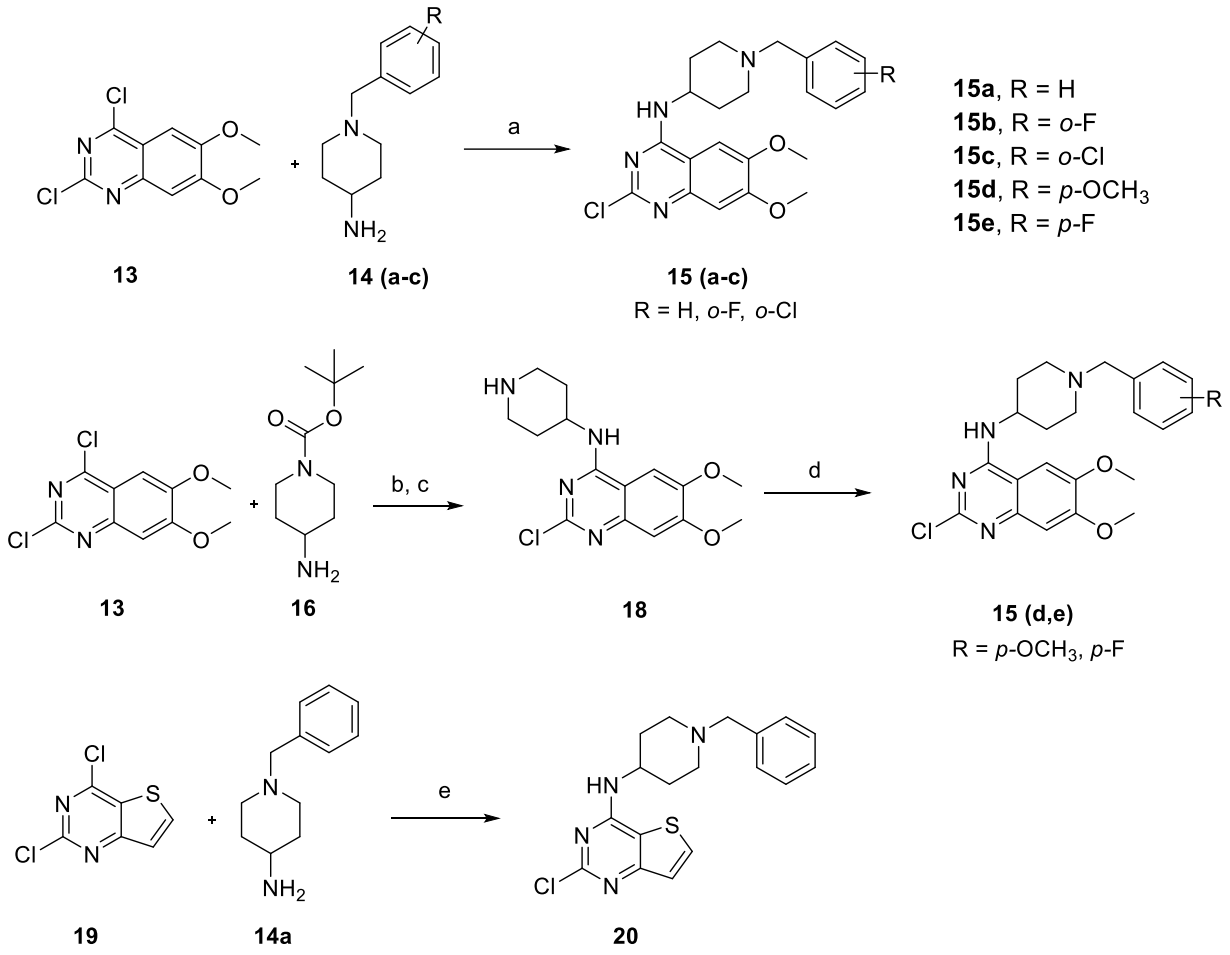

(a) THF, DIPEA, 50°C, 3h, 36-76%; (b) THF, DIPEA, 50°C, 3h, 71%; (c) CH_3COCl, MeOH, 0°C to RT, 4h, 96%; (d) RBnCHO, $NaCNBH_3$, AcOH, MeOH, RT, 16 h, 46-75%; (e) DIPEA, THF, 50°C, 4h, 76%.

Scheme 2. Synthesis of quinazoline and thienopyrimidine precursor

Aromatic nucleophilic substitution of precursors **15a-e** and **20** with amines **9**, **12** and **21** required strong acidic conditions in a sealed tube achieved with 4 M HCl in dioxane at 130 °C.[33] The products were obtained as a mixture of methyl and *iso*propyl esters which was inconsequential since the subsequent steps necessitated their saponification to the respective carboxylic acids. Straight chain HDACi precursor **21** did not react with **15a** under acidic sealed tube conditions. However, the coupled product was obtained in high yield (86%) when the reaction was conducted under basic conditions using di*iso*propylethylamine (DIPEA). Esters **22a-h** were hydrolysed to the corresponding acids **23a-h** using an excess of LiOH.[39] Following

an extraction procedure to remove the unreacted ester, the carboxylic acid intermediates were converted to hydroxamic acids via tetrahydropyran-2-yl-protected hydroxyl amine (THP-NHOH) giving intermediates **24a-h**. HATU/TEA mediated acid-amine coupling underwent smooth conversion resulting in 56-93% yields after purification by column chromatography (DCM/MeOH + 0.002% NH_4OH).[39] The THP group was deprotected in the presence of 4 M HCl/dioxane overnight to afford the target compounds **25a-h**.[39] In most cases, the final deprotection reaction did not undergo completion resulting in small amounts of starting material in the product. The crude products were triturated with DCM or DCM/MeOH (99:1). Several factors such as solubility, basicity and polarity posed challenges in purification by column chromatography. Therefore, most of the final products were purified by preparative reverse phase HPLC resulting in highly variable yields (6-97%).

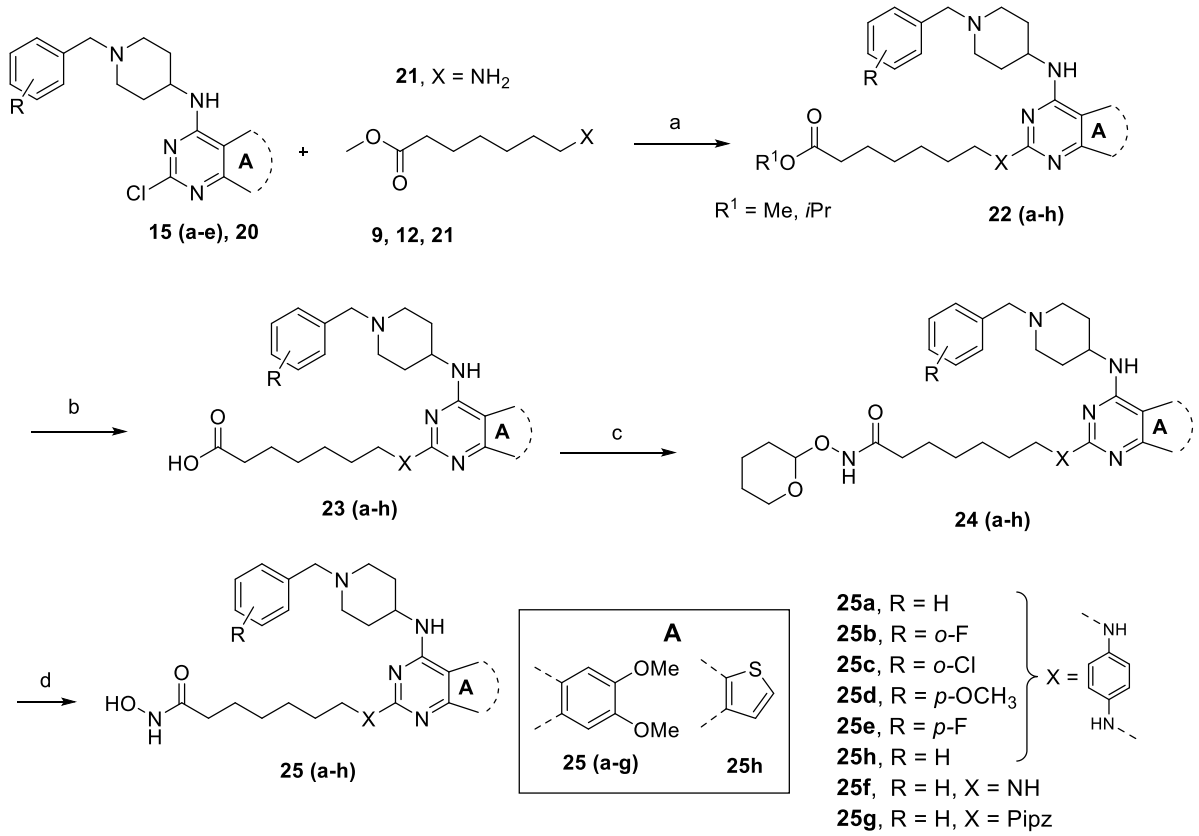

(a) IPA, 4M HCl/Dioxane, ST, 135°C, 4-5 h, 25-86%; (b) LiOH, THF/water (2:1), 50-70°C, 6-10 h, 33-71%; (c) Tetrahydropyran-2-hydroxyl amine, HATU, TEA, DMF, RT, overnight, 56-93%; (d) THF/Dioxane, TFA, overnight, 6-97%.

Scheme 3. Coupling of precursors leading to the generation of hydroxamic acid moieties **25a-h**

Assessment of Compounds Against Isolated Enzymes

Compounds were tested against two HDAC isoforms, HDAC1 and HDAC6, using an HDAC enzyme assay.[40] HDAC1 is a representative of class I HDACs and HDAC6 (class IIB) is an isoform known to be sensitive to molecules that form interactions with the edge of the Zn binding pocket.[22–24] The synthesized molecules displayed low nanomolar IC_{50} values against HDAC6 whereas potencies against HDAC1 were found to be 50-100 fold lower (

Table 1). Compound **25a** was found to be the most potent compound in the series with sub-nanomolar potency against HDAC6 (0.5 nM) and 2,000-fold selectivity against HDAC1 (1.03 µM). **25a** was also found to be 40 times more potent than **3** against HDAC6.

Table 1. HDAC1 and HDAC6 inhibition data for **25a-h**

Compound	HDAC1 IC_{50}	HDAC6 IC_{50}	HDAC1/HDAC6

	(nM)	(nM)	ratio
3	306	20	15
TSA	6.22	1.94	3
25a	1030	<0.5	2060
25b	1060	3.87	274
25c	3370	9.09	371
25d*	896 ± 47	2.6 ± 1.8	345
25e	2150	7.98	269
25f	798	32.3	25
25g	3080	35.5	87
25h	233	5.9	40

TSA, Trichostatin A. All compounds were tested in a 10 concentration dose response. *For compound **25d**, IC_{50} data are reported as the average of two independent 10-point dose response determinations as the molecule was used for further studies.

The majority of the pyrimidine analogues, **25b-e**, led to a drop in the HDAC6 potencies by 5-18 fold compared with **25a**. However, these compounds displayed improved HDAC6 potency compared to **3**. Against HDAC1, most compounds were less active than **3** with the exception of the thienopyrimidine **25h** which was slightly more active with an IC_{50} value of 233 nM. Modifications to the HDACi pharmacophore (**25f** and **25g**) were not well tolerated and led to lower potencies, thus highlighting the importance of the anilide group for HDAC inhibitory activity. HDAC1/HDAC6 selectivity has been calculated for each compound (Table 1). There are several compounds with high HDAC6 selectivity (>200 fold). We were interested in further studying compounds with high selectivity for HDAC6 and with antiproliferative effects (discussed in the next section) similar to the reference standards. This data suggests that **25d**, with high potency for HDAC6, high selectivity for HDAC1, and good anti-proliferative effects in two cancer cells, would be a suitable candidate to explore further.

Table 2. Isoform selectivity of **25d** against Class I, II, and IV HDAC Enzymes

Enzyme isoform	Class	IC_{50} (µM) or % Inhibition	HDAC6 SI
HDAC1*	I	0.9 ± 0.1	345
HDAC2	I	1.1	435
HDAC3*	I	0.034 ± 0.001	13
HDAC4	IIA	20% at 10 µM	>3000
HDAC5	IIA	25% at 10 µM	>3000
HDAC6*	IIB	0.0026 ± 0.002	1
HDAC7	IIA	NA[#]	NA[#]
HDAC8	I	1.26	485
HDAC9	IIA	21% at 10 µM	>3000
HDAC10	IIB	2.69	1035
HDAC11	IV	1.81	696

*IC_{50} data are reported as the average of two independent determinations. [#]No inhibition at 10 µM concentration of **25d**. SI = Selectivity Index.

Compound **25d** was selected as a representative of the series for further characterisation against a panel of 11 HDAC enzymes (

Table 2). To our surprise, a unique selectivity for the HDAC3 enzyme was revealed, in addition to HDAC6, with a potency of 34 nM. Potency against other isoforms was around 1 µM or above. No activity at up to 10 µM concentration was observed against the Class IIA isoforms HDAC4, HDAC5, HDAC7, HDAC9.

Several chemical classes of HDAC6 and HDAC3 inhibitors, as well as HDAC1/3, HDAC6/8 dual inhibitors have been reported.[41–47] Compound **25d** however displays a unique and unprecedented HDAC3/6 selectivity.

Table 3. Testing **25d** against Methyltransferase enzyme panel

Enzyme	**Methylation site**	**IC_{50} (μM) or % inhibition at 100 uM**
DNMT1*	CpG	14 ± 4
DNMT3a*	DNA including non-CpG sites	74 ± 34
DOT1L	H3K79	16%
EZH2 Complex	H3K27	27%
G9a H3(1-21)	H3K9, H3K27	37%
MLL1 Complex	H3K4	42%
PRMT1	H4R3	NA
SET7/9	H3K4	19%
SUV39H1	H3K9	14%
SUV39H2	H3K9	NA
G9a IC_{50} for reference standards (μM)	**1**	2.01
	2	0.026

*IC_{50} data are reported as the average of two independent determinations.

Having established the HDAC selectivity profile, we tested **25d** against a panel of 10 methyltransferases (

Table 3).[48] Surprisingly, **25d** only weakly inhibited G9a (37% at 100 μM) and was found to be most potent against DNMT1 (DNA methyltransferase) with an IC_{50} of 13.95 μM and DNMT3a to a lesser extent (IC_{50} = 73.6 μM). These results are in agreement with studies based on specific chemical modifications at the C-2 position of desmethoxy-**1** leading to loss of G9a inhibitory activity while gaining selectivity towards DNMT3A.[49] The activities against other methyltransferases were not significant even at the highest concentration of 100 μM.

Modelling Studies

The *in vitro* assays against the panel of HDAC isoforms revealed a unique selectivity profile of **25d** with nanomolar potency against HDAC3 and HDAC6. It is especially interesting that **25d** displayed isoform selectivity for HDAC3 (34 nM) compared with other class I HDACs (~1 μM against HDAC1 and HDAC2). To understand the selective binding of the compound against HDAC6 and HDAC3, we performed docking studies of **25d** to various HDAC isoforms (**Figure 4A**).

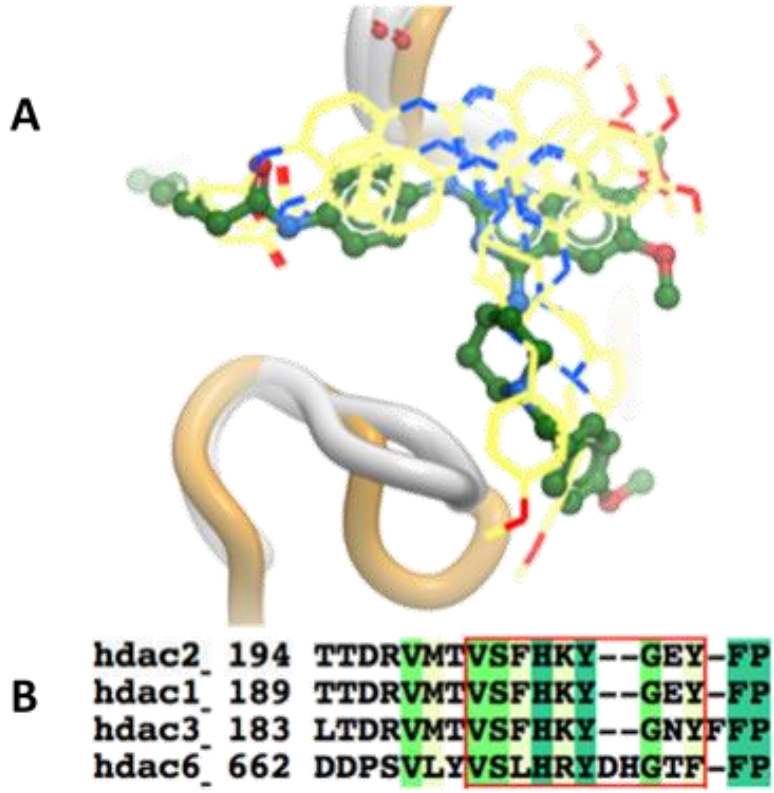

Figure 4. A) Comparison of **25d** docking against HDAC1 (PDB id 4BKX), HDAC2 (PDB id 5IWG), HDAC3 (PDB id 4A69) and HDAC6 (PDB id 5EDU) isoforms. **25d** binding to HDAC6 is coloured green, while the bound orientation in HDAC1, 2 and 3 are coloured yellow; B) Sequence comparison of HDAC6 versus Class I HDACs shows the presence of two extra residues (aspartic acid and histidine) that impart additional flexibility.

There are two extra residues (**Figure 4B**) present in a loop at position 675 and 676 in HDAC6 (PDB ID: 5EDU chain B; coloured orange), which are not present in HDAC1, 2 or 3 (coloured white). This imparts additional flexibility to the loop, along which **25d** can effectively bind to. The lack of two additional residues constrains this loop in HDACs 1, 2 and 3 which explains the exceptional potency of **25d** against HDAC6.

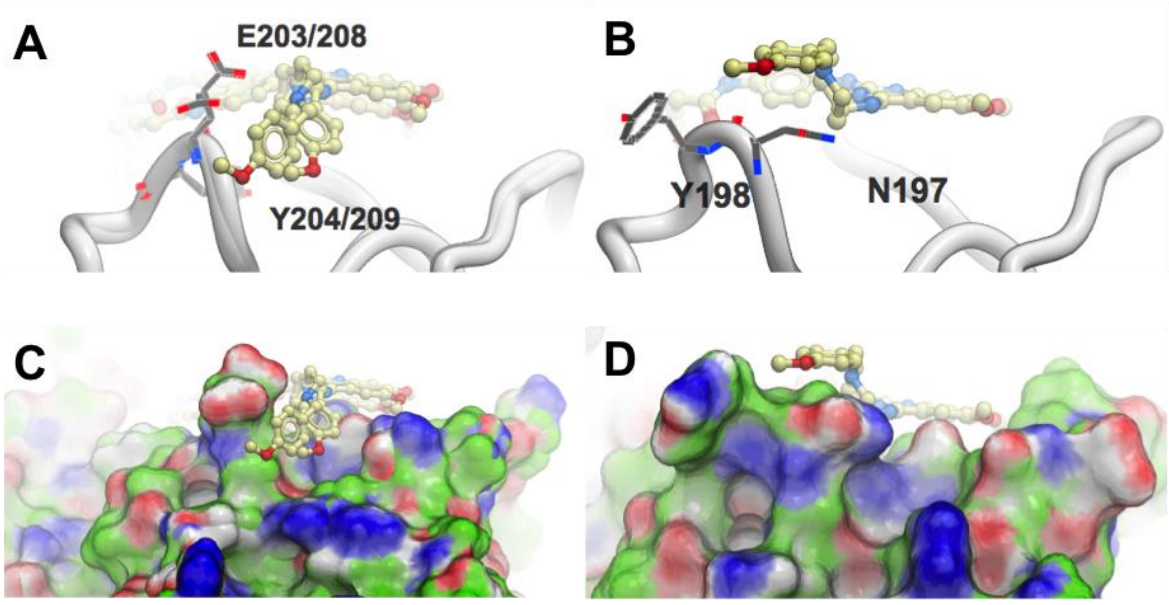

Figure 5. Docking of **25d** to understand potency differences within Class I HDACs (HDAC3 versus HDAC1 and 2). A) Just following the loop, there is a sequence and structural conservation of residues in HDAC1 (E203, Y204) and 2 (E208, Y209); B) Although a tyrosine residue is present at Y198 in HDAC3, the side chain is not in the same orientation as in HDAC1 and 2. Additionally, an asparagine replaces glutamic acid at position 197 in HDAC3; C) The side chains of glutamic acid in HDAC1 and 2 are oriented vertically upwards, which forces the side chain to position laterally along the loop; D) However, the side chain of N197 lies horizontal to the loop in HDAC3 The side chain of **25d** is not long enough to bypass this orientation, but effectively stacks on the loop. (PDB ids HDAC1 – 4BKX; HDAC2 – 5IWG; HDAC3 – 4A69)

Further detailed modelling studies illuminate the differences in key compound binding residues between the Class I HDAC isoforms that explain the selectivity against HDAC3 (**Figure 5**). Within these isoforms, the orientation of asparagine residue N197 in HDAC3 is notably different from HDAC1 and 2 which have a glutamic acid at the same position. This results in significant differences in the conformation of the loop (**Figure 5D**) leading to a preferred conformation of **25d** when bound to HDAC3, plausibly explaining **25d** being 26-33 fold more potent against HDAC3 compared with HDAC1 and 2.

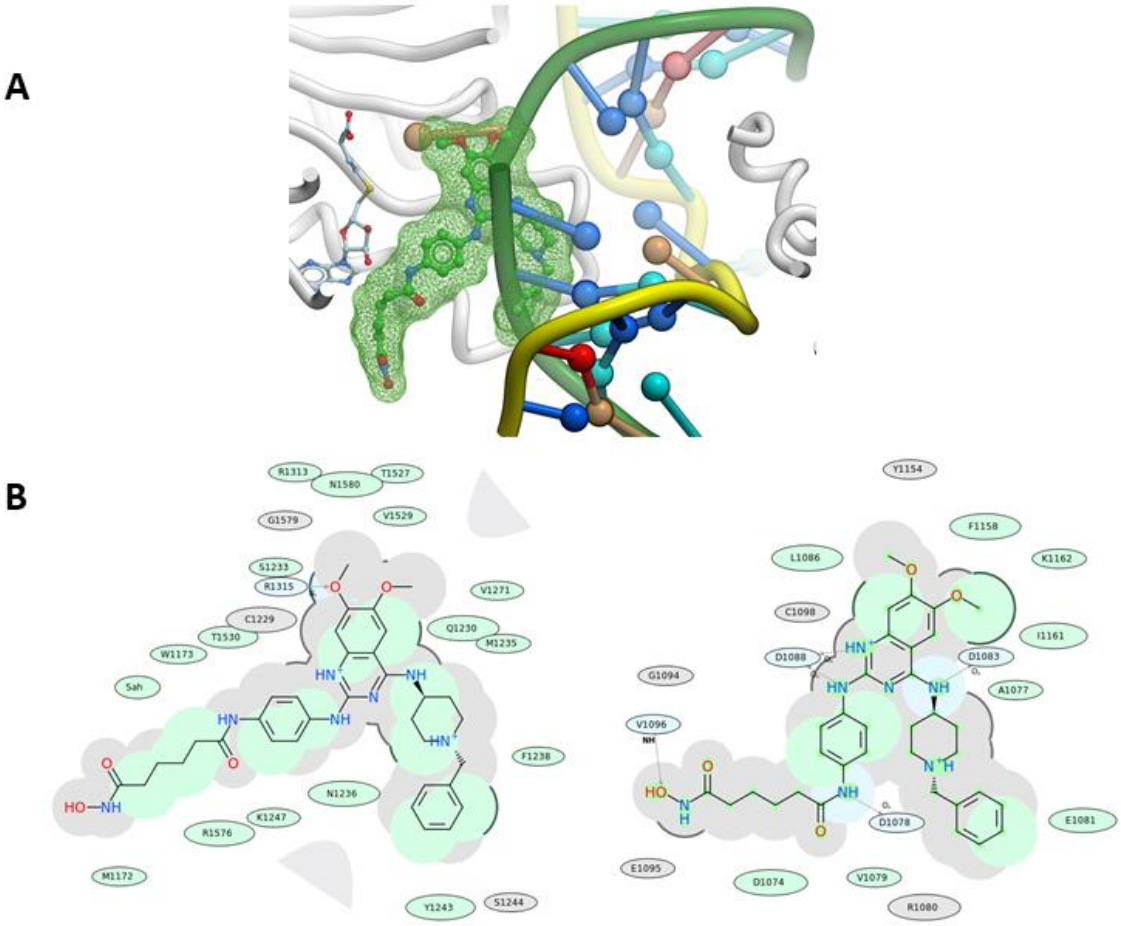

Figure 6 A) **25d** binding superimposed on the DNMT-DNA complex (PDB ID: 4DA4 structure). The binding site of **25d** sits adjacent to S-Adenosyl-L-homocysteine (SAH) and overlaps with the DNA binding region; B) 2D cartoon plots depicting **25d** binding to DNMT (left) and G9a (right).

Further to understanding HDAC isoform selectivity, we also sought explanation for the preferential binding of **25d** to DNMT binding compared with G9a MT. The 2D plots of **25d** binding in the two sites have been illustrated. In the DNMT-**25d** complex, **25d** occupies the pocket where DNA is bound in the apo structure and lies adjacent to the SAH co-factor. It is plausible that **25d** competes with DNA binding to DNMT and therefore exhibits a greater affinity to DNMT than G9a. In the G9a-**25**d complex, 25d does not occupy the lysine binding

channel which probably explains the lack of binding potency towards G9a in the biochemical assays.

Assessment of Compounds in Proliferating Breast Cancer Cells

Lee et al have demonstrated via a series of experiments that silencing HDAC3 and HDAC6 induced the downregulation of survival protein, Survivin, leading to the loss of viability of breast cancer cells MCF-7 and MDA-MB-231.[50] This, coupled with the established activities of G9a and HDAC inhibitor reference compounds on these cell lines, motivated us to perform antiproliferative assays of the synthesised compounds on MCF-7 and MDA-MB-231 cells.[9,51] An MTT assay, which assesses mitochondrial cell death, was employed to evaluate the anti-proliferative efficacies of the molecules. The compounds exhibited similar IC_{50}s in the range of 2-11 μM against both cell lines (

Table 4).

Modifications of the benzyl group showed little preference to the nature, type and position of the substitutions. The compounds were found to be 2-3 fold less potent compared with both the positive controls **1** and **3**. Interestingly, the scaffold-hopped thienopyrimidine, **25h**, showed potency similar to the reference standard **1** (2.8-2.9 μM).

Table 4. Cell proliferation inhibition data of compounds against two breast cancer cell lines

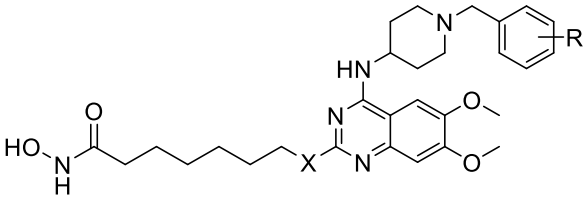

25a-g

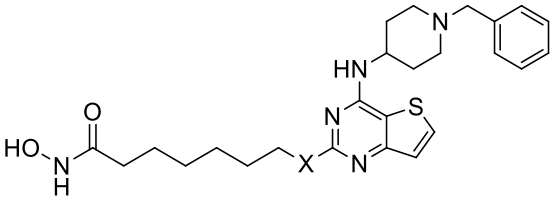

25h

Compounds	R	X Linker	MDA-MB-231 IC_{50} (μM)	MCF-7 IC_{50} (μM)
1	-	-	2.9 ± 0.3	3.3 ± 0.4
3	-	-	1.2 ± 0.2	0.65 ± 0.1
25a	H	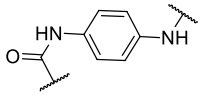	5.1 ± 0.5	12 ± 1
25b	*o*-F	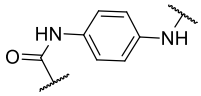	6.1 ± 2.3	2.1 ± 0.6
25c	*o*-Cl	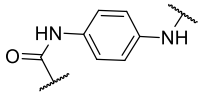	4.1 ± 0.5	4.9 ± 0.8
25d	*o*-Me	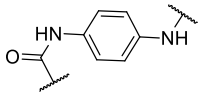	6.3 ± 1.4	7.3 ± 1.1
25e	*p*-F	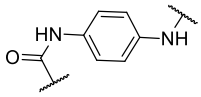	4.9 ± 1.4	4.9 ± 1
25f	H	NH	11 ± 1.3	9.5 ± 4
25g	H	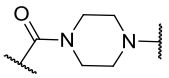	7 ± 1.4	7.7± 1.3
25h	H	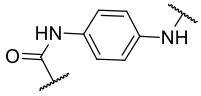	2.9 ± 1.2	2.9 ± 0.9

On the other hand, modifications to the hydroxamate bearing side chain were less favoured, specifically the straight chain derivative **25f**. While **25g** has antiproliferative activity similar to other molecules in the series, **25f** showed a 2-3 fold drop in the IC_{50} values – possibly

indicating the importance of either a cyclic connection or a specific distance between the quinazoline and hydroxamate moiety. However, since effects on the cell cycle and cell death are a complex interplay of events, a 2-3 fold difference in the activities was not considered to be conclusively different.

Apart from breast cancers, HDAC meditated histone acetylation is one of the molecular hallmarks in hematological malignancies.[52] For example, HDAC6 and HDAC3 are overexpressed in Mantle Cell Lymphoma (MCL), and mice which have a germline knockout of HDAC6 displayed significantly reduced tumor progression compared to the wild-type mice. Additionally, genetic or pharmacologic disruption of HDAC3 also resulted in decreased cell proliferation, increased apoptosis and reversal of the drug-resistance phenotype of MCL cells.[53] We therefore took the opportunity to perform a preliminary screening of compound **25d** against multiple myeloma and acute myeloid leukemia cell lines (**Table 5**) due to the established high expression of HDACs and demonstrated value of HDACi in treating these cancers.[54] Although **25d** was found to be 3-8 fold less potent than **3**, given the HDAC enzyme selectivity profile (

Table 2), it would be worthwhile to study the pharmacodynamics of **25d** in affecting the acetylation levels in these cells.

Table 5. Cell proliferation inhibition data of **25d** against four haematological cell lines

Compound	KMS-12-BM IC_{50} (μM)	H929 IC_{50} (μM)	OPM2 IC_{50} (μM)	MOLM14 IC_{50} (μM)
3	0.9 ± 0.2	1.4 ± 1	2.9 ± 0.9	0.5 ± 0.1
25d	7.6 ± 1.8	4.6 ± 0.2	7.9 ± 0.4	2.8 ± 0.8

NT = not tested. KMS-12-BM, H929, and OPM2: multiple myeloma cell lines; MOLM14: acute myeloid leukemia cell line

Mechanism of cell death in cancer cells

Following the phenotypic studies on various cancer cell lines, we aimed to gain an understanding on the mechanistic aspects of cell death induced by these compounds. We investigated if apoptosis was a likely mechanism of cell death. Cell death is preceded by specific events like the translocation of phosphotidylserine (PS) to the outer plasma membrane, eventually leading to loss of integration of the cellular structure. Annexin V, a Ca^{2+} dependent protein, has a high affinity for PS and binds to the exposed PS which marks early apoptosis. When used in conjunction with propidium iodide – which is specific to late apoptosis – this assay distinguishes between cells in early and late apoptosis as well as dead cells (stained by both Annexin V and PI).

Compound **25d** was studied at 3 different concentrations (0.5 x IC_{50}, IC_{50} and 1.5 x IC_{50}) to examine effects on apoptosis in MDA-MB-231 breast cancer cells. Doxorubicin was used as a positive control. Treatment with **25d** resulted in an increase in the population of Annexin V stained cells (Q4, 18-24%) compared with untreated cells (~5%). A concentration-dependent response was not evident, although early apoptosis (Q4, Annexin V+, PI-) predominates at all three concentrations of **25d** (**Figure 7**). These results further corroborate the studies by Lee et al, who demonstrated that specific targeting of isoforms HDAC6 and HDAC3 in breast cancer cells (MDA-MB-231 and MCF-7) leads to autophagy by inducing downregulation of survivin – a potent inhibitor of apoptosis.[50]

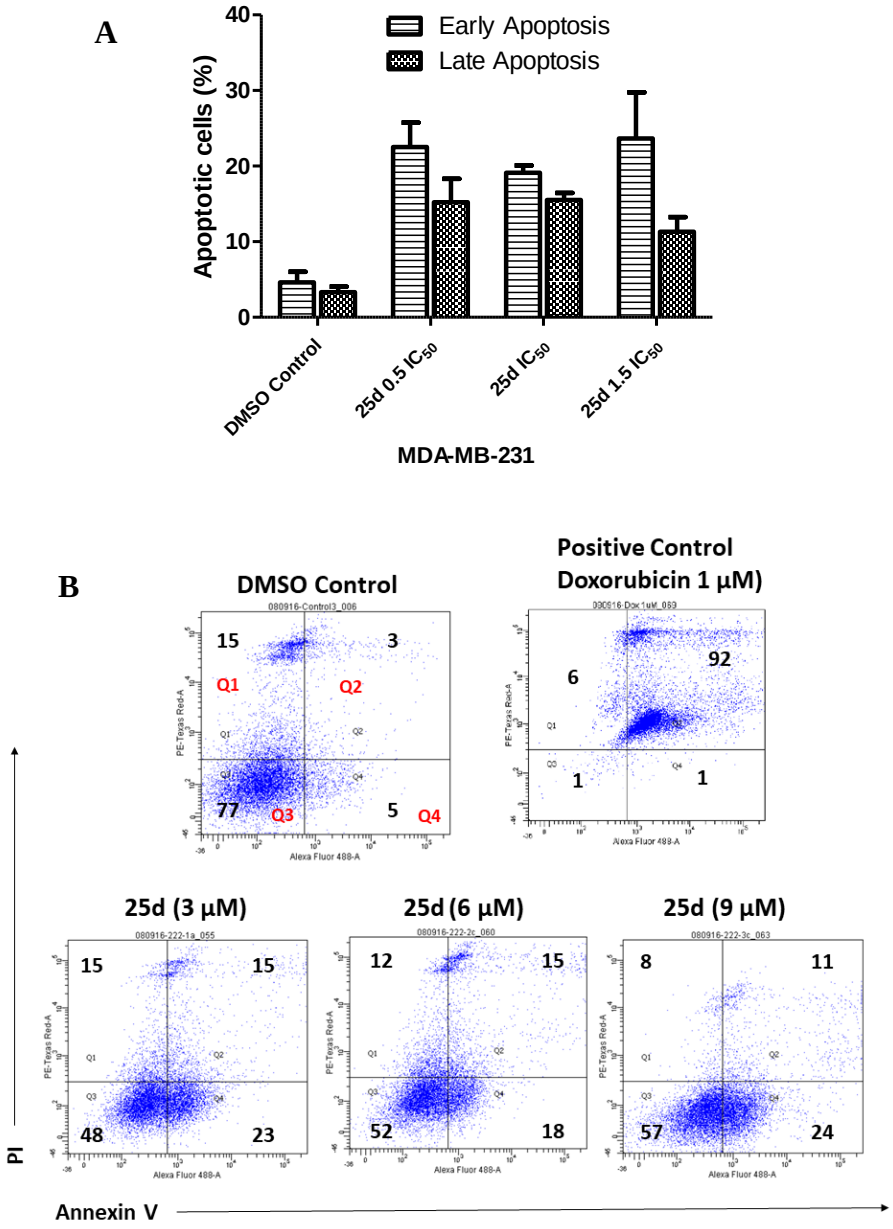

Figure 7. Study of apoptotic effects on breast cancer cell line (MDA-MB-231) after 48 h treatment with **25d**. A) Percentage of early apoptotic cells are highest at all three concentrations (0.5 x IC_{50}, IC_{50} and 1.5 x IC_{50}) of **25d**; B) Annexin V FITC vs PI plots from the gated cells show the populations corresponding to viable and non-apoptotic (Q3, annexin V−PI−), early apoptic (Q4, annexin V+PI−), late apoptotic (Q2, annexin V+PI+) cells and dead cells (annexin V-PI+).

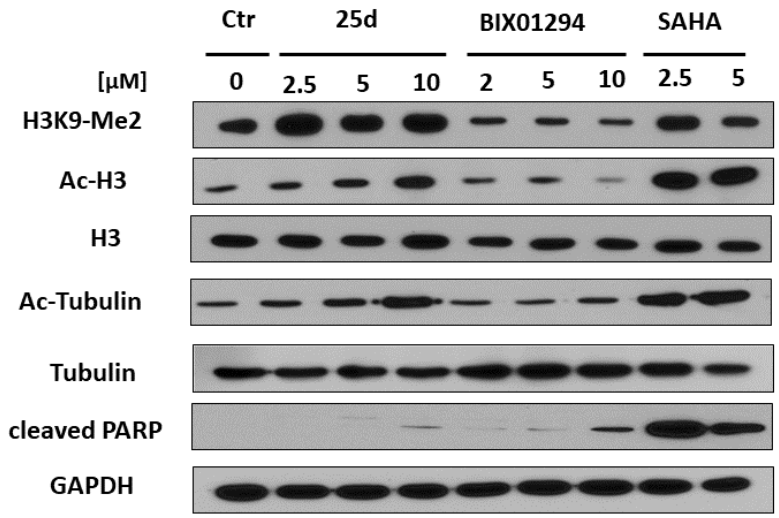

Figure 8. Immunoblotting analysis of multiple myeloma cell line KMS-12-BM after 24 h treatment with indicated concentrations of compounds **25d**, **1** and **3**. Effects of **25d** treatment on protein expression levels of H3K9 methylation, Histone 3 acetylation, tubulin acetylation and cleaved PARP were studied.

To study the intracellular mechanism of action of **25d** and its effect on pharmacodynamic biomarkers for methylation and acetylation, we conducted immunoblotting assays against KMS-12-BM (multiple myeloma) cell lines (**Figure 8**). Both reference standards, **1** and **3**, were used for analysing effects on methylation (H3K9Me2) and acetylation (Ac-H3 and Ac-Tubulin) levels, respectively. Levels of Ac-H3, regulated by HDACs 1, 2 or 3, increased markedly in a concentration-dependent manner with **25d** (IC_{50} = 7.5 μM) treatment. This was concurrent with an increase in Ac-tubulin levels, which is specifically mediated by isoform HDAC6. Interestingly, **1** was found to act in the reverse direction by decreasing Ac-H3 levels. Compound **3**, was used as a positive control and increased both Ac-H3 and Ac-tubulin levels as expected. These results are in agreement with the *in vitro* HDAC assay results which indicate selective nanomolar potent inhibition of HDAC3 and HDAC6 by **25d**.

With regards to H3K9Me2 levels, the positive control **1** (MT inhibitor) displayed significant inhibitory effects as reported previously.[55] Interestingly, pan-HDACi **3** as well as **25d**

increased H3K9Me2 levels. To achieve our original hypothesis of dual target inhibition activity, H3K9Me2 levels must decrease and Ac-H3 and Ac-tubulin levels must increase. Our immunoblotting studies indicate that methylation levels are increasing upon HDAC inhibition, thereby indicating the potential for synergy on combining with a H3K9 specific methyltransferase inhibitor. Effects on cleaved PARP upon treatment with **25d** were only just detectable at the highest concentration tested. This suggests that apoptosis is occurring and is consistent with the Annexin/PI studies.

Cheng et al. have previously demonstrated that selective inhibition of HDAC6 and HDAC3 – both enzymes that play a key role in apoptosis – offers a promising therapeutic strategy for the treatment of mantle cell lymphoma.[53] Our preliminary research on the effects of **25d** on hematological cell lines coupled with biochemical assays implicating HDAC3/6 selectivity, strongly encourages further investigation on its potential against mantle cell lymphoma.**Error! Bookmark not defined.**

In vitro ADME testing revealed **25d** to have low kinetic solubility but high effective permeability (P_e) (**Table 6**). *In vitro* metabolic studies were performed in both rat and mouse liver microsomes (RML and MLM¸ **Table 6**). **25d** was found to metabolise slowly in both species of RLM with an intrinsic clearance of 22.3 (female) and 16.3 (male) µL/min/mg (

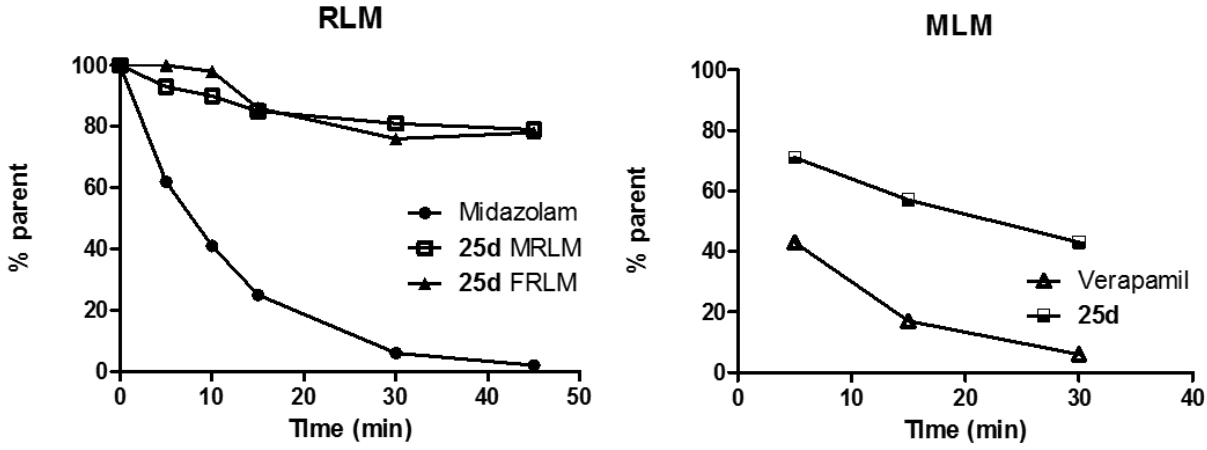

Figure 9). In MLM, **25d** displayed a moderate clearance with a value of 52.2 µL/min/mg (

Table 6).

While anticancer drugs are associated with a variety of off target toxicities, drug induced cardio and hepatotoxicity pose considerable hurdles in oncology drug development. We performed *in vitro* toxicity assessments against normal hepatocytes and cardiomyocytes to assess their propensity to damage the heart and the liver. We were pleased to discover that **25d** displayed much higher IC_{50}s against these normal cells demonstrating a therapeutic window of between 4 and 13-fold (

Table 7). Furthermore, an AMES test was performed against *Salmonella typhimurium* to detect if the drug can cause mutations on the histidine residues that would classify it as a potential carcinogen; **25d** was found not to produce any genotoxic effects. Overall, the preliminary pharmacokinetic and toxicity findings were generally favourable and encourage future *in vivo* characterisation of the compound.

Table 6. *In vitro* ADME analysis of **25d**

Parameter		Results	
Kinetic Solubility		At 3 h: 4.6 ± 0.3 µM 3.0 µg/mL	At 24 h: 4.0 ± 0.3 µM 2.60 µg/mL
Permeability (10^{-6} cm/s)[a]		21.8 ± 5 (6h)	7.9 ± 2.7 (16h)
MLM[b]	$t_{1/2}$ (min)	26.6	
	Cl_{int} (µL/min/mg)	52.2	
RLM[b]	$t_{1/2}$ (min)	103.6 (female), 143.1 (male)	
	Cl_{intr} (µL/min/mg)	22.3 (female), 16.3 (male)	

[a] Parallel Artificial Membrane Permeability Assay (PAMPA); [b] Mouse or rat liver microsomes, half-life or intrinsic clearance.

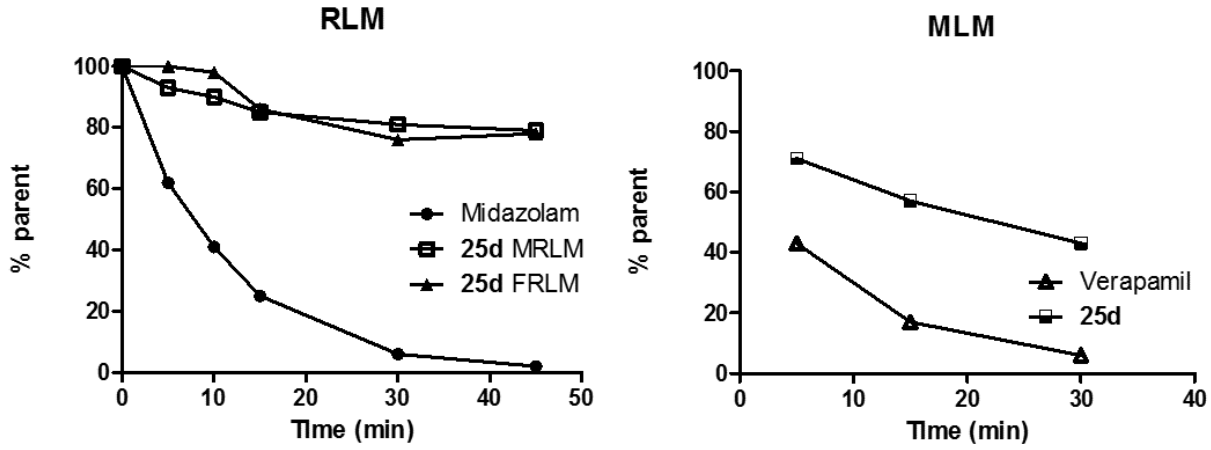

Figure 9. Metabolism of **25d** A) Percentages of remaining **25d** and positive control midazolam relative to initial amounts (t = 0) in male and female rat liver microsomes upon incubation at 37 ºC for 5, 10, 15, 30 and 45 min; B) Percentages of remaining **25d** and positive control verapamil relative to initial amounts (t = 0) in mouse liver microsomes upon incubation at 37 ºC for 5, 15, and 30 min.

Table 7. Toxicity analysis of **25d** in normal cells

***In vitro* system**	**IC_{50} (µM)**	**Therapeutic Window (ratio of toxicity IC_{50}/cancer cell IC_{50})**
TAMH	29 ± 0.6	4
AC-10	94 ± 8	14
Genotoxicity (AMES test)	No effect	-

The application of epigenetic targeted inhibitors spans a number of therapeutic areas and extends to infectious diseases like malaria.[4] Growing evidence suggests the involvement of epigenetic mechanisms in the survival of different *Plasmodium* species and are being studied as a potential treatment for malaria. Similar to human physiology, PTMs like methylation and deacetylation play an important role in the life cycle of *P. falciparum* - one of the most infectious malarial strains. These PTMs empower the parasite by enhancing their ability to invade human red blood cells as well as to evade the immune system.

Epigenetic inhibitors including HDACi (hydroxamates and nicotinamide-based compounds) and more recently G9a inhibitors (such as **1**) have been studied for their antimalarial efficacies.[56,57] Antimalarial drug resistance is one of the critical issues of concern.

We tested a subset of the synthesized inhibitors against 3D7 and K1 strains using chloroquine as the reference standard (**Table 8**). On CQ-sensitive 3D7, all compounds were found to be 3-6 fold (95-200 nM) less active than chloroquine. On the other hand, most compounds were found to be as potent (292-878 nM) as the reference standard against the K1 strain, with **25e** being the most potent of the series. Although the dual inhibitors were found to be less potent than the reference CQ against 3D7, they displayed meaningful activities particularly against CQ-resistant malarial strains and much lower resistance (ratio K1/3D7). This proof-of-concept study has provided encouraging results and provided a justification for further investment in the exploration of the potential of this series of selective HDACi as a strategy for combating antimalarial drug resistance.

Table 8. Anti-malarial efficacies of compounds against *P. falciparum*

Compound	3D7 IC_{50} (nM)	K1 IC_{50} (nM)	Resistance Ratio K1/3D7
Chloroquine (CQ)	34 ± 3	457 ± 58	14
1	152 ± 8	180 ± 3	1
3	274 ± 49	262 ± 50	1
25a	200 ± 50	878 ± 245	3
25b	98 ± 42	611 ± 82	6
25c	96 ± 11	489 ± 74	5
25d	145 ± 20	508 ± 50	4
25e	111 ± 34	296 ± 47	3

Concluding remarks

Employment of a pharmacophore merging strategy of two epigenetic targeted inhibitors led to the serendipitous discovery of a series of novel small molecules displaying an unprecedented selectivity profile against two HDAC isoforms. The series was found have low nanomolar potency against HDAC6 as revealed by *in vitro* biochemical assays. A preferred molecule, **25d**, following profiling in a panel of HDACs, was found to have low nanomolar potency against HDAC3 and HDAC6 with 300-3000 fold selectivity against other HDAC isoforms. Any alterations to the HDACi pharmacophore were not tolerated and led to about 30-fold reduced HDAC6 potencies. While testing of **25d** in a methyltransferase panel nullified our initial hypothesis of activity against G9a, mild inhibition of DNMT1 was observed. The series of compounds **25a-h** displayed low micromolar *in vitro* antiproliferative activities against two types of breast cancer cells as well as four hematological cell lines. Further studies with **25d** showed early apoptosis as one of the mechanisms of cell death in MDA-MB-231 breast cancer cells. Immunoblotting studies on KMS-12-BM multiple myeloma cells with **25d** was found to increase levels of all three biomarkers: Ac-H3, Ac-tubulin as well as H3K9Me2. These results

suggest that inhibition of both G9a and HDACs could have synergistic effects. Modelling studies identified the role of two extra residues in HDAC6 in imparting additional flexibility for **25d** binding further corroborating the potency trends observed with *in vitro* biochemical assays. *In vitro* pharmacokinetics and toxicological profiles of **25d** were generally favourable and warrant further studies *in vivo*. Investigation of the molecules in *plasmodium* species revealed potent antimalarial effects particularly in CQ-resistant strains (K1), thus presenting potential application of these compounds in drug-resistant malaria. Our exploratory research provides a starting point for studies of selective HDAC3/6 inhibitors in multiple therapeutic domains.

EXPERIMENTAL SECTION

Chemistry and Synthesis

General Remarks: All chemicals and solvents were procured from commercial sources (Sigma, Scientific Resources, Tee Hai Chemicals, Reagent Chemicals, Ark Pharma, Combi block), and were used without further purification.

All the structures and their IUPAC names have been generated using ChemBioDraw Ultra 15.0. The numbering of the atoms in compounds have not followed IUPAC norms, but followed a logical sequence according to the synthesis of the compounds.

Reactions and purifications: Reactions were carried out in oven-dried round bottom flasks under inert nitrogen atmosphere in order to prevent degradation by moisture or oxygen. All reaction temperatures stated in the procedures are external bath temperatures. Microwave reactions were performed in Biotage microwave reactor. Silica coated aluminium sheets from Merck were used for monitoring reactions by thin layer chromatography (TLC), and the spots were examined under UV light and using $KMnO_4$ stain solution with heating. The retardation

factor (R_f) of the compounds have been calculated with respect to the solvent front and have been reported in the following manner: R_f = value (elution system).

All products were purified by flash chromatography using silica gel as the stationary phase, unless specifically stated otherwise. The purifications of most of the final compounds, and polar intermediates (with basic centers) have used 0.5% TEA or 0.2% NH_4OH to prevent any decomposition/retention by the acidic silica gel. Reverse phase purification of samples was done using preparative HPLC, Agilent technologies using standard gradient over 20 min (MeCN/Water = 5:95 to 95:5).

Analysis: Nuclear Magnetic Resonance (NMR) spectra were recorded on a Bruker Spectrospin Ultrashield spectrometer, using 400 MHz for ^1H NMR and 100 MHz for ^{13}C NMR. The chemical shifts are reported in ppm (δ), relative to solvent $CHCl_3$ (7.26 ppm), CD_3OD (3.31 ppm), $(CD_3)_2SO$ (2.5 ppm) with ^1H NMR; $CHCl_3$ (77.16 ppm), CD_3OD (49.00 ppm), $(CD_3)_2SO$ (39.52 ppm) in ^{13}C NMR. Multiplicities are reported as follows: singlet (s), doublet (d), triplet (t), multiplet (m), broad singlet (bs). Coupling constants (J) are reported in Hz. The unit of molecular weight reported is $gmol^{-1}$. The attributions in ^{13}C NMR spectra have been done based on ^{13}C DEPT and predicted chemical shifts on ChemDraw 12.0.

Low resolution mass spectra were obtained on an Agilent 6130B quadrupole LC/MS in ESI mode with an Agilent 1260 Infinity LC system using a ThermoScientific Hypersil 150 mm × 2.1 mm 5 μm column or a Shimadzu LCMS-2020 in ESI mode. Analytical HPLC purity profiles were obtained using Agilent technologies 1200 series.

Procedure for suberic acid monomethyl ester aromatic amides

In an RBF, suberic acid monomethyl ester (1.43 g, 7.58 mmol, 1 equiv.) was dissolved in 15 mL DCM and N-methyl morpholine (1 mL, 9.09 mmol, 1.2 equiv.) was added to the reaction mixture and allowed to stir at 0^0C. Ethyl chloroformate (0.689 mL, 7.20 mmol, 0.9 equiv.) was

added from a dropping funnel under nitrogen atmosphere. After 0.5 h, **7** in DCM (1.5 g, 7.203 mmol, 0.95 equiv.) was added and allowed to stir overnight. The reaction was monitored via TLC under UV and $KMnO_4$ for completion, was quenched with water and extracted with DCM (30×3 mL). The combined organic layers were washed with brine, dried over anhydrous sodium sulphate, and concentrated under reduced pressure to give a solid residue. The crude residue was purified by flash chromatography (elution system- Hex/EA = 40:60 to 20:80) to obtain 2.28 g (84%) compound **8** as a pale white solid.

Methyl 8-((4-((tert-butoxycarbonyl)amino)phenyl)amino)-8-oxooctanoate (**8**)

R_f = 0.39 (Hex/EA = 1:1). **^{1}H NMR** (400 MHz, $CDCl_3$) δ (ppm) = 7.60 (bs, 1H), 7.4 (d, *J* = 10.4 Hz, 2H), 7.27 (d, *J* = 7.0 Hz, 2H), 6.65 (bs, 1H), 3.64 (s, 3H), 2.30-2.26 (m, 4H), 1.70-1.58 (m, 4H), 1.49 (s, 9H), 1.35-1.31 (m, 4H).

General Procedure for suberic acid ester aliphatic amides

To a solution of mono-Boc protected piperazine (50 mg, 0.224 mmol, 1 equiv.) in DCM, was added suberic acid monomethyl ester (48.2 mg, 0.270 mmol, 1.2 equiv) and NMM (74 μL, 0.67 mmol, 3 equiv). This was followed by the addition of coupling agents EDC (69.4 mg, 0.45 mmol, 2 equiv) and HOBt (51.4 mg, 0.34 mmol, 1.5 equiv), and the reaction was allowed to at room temperature for 4 h. After completion, the reaction was washed with water (15 mL), and the aqueous layer was further extracted with DCM (25×3 mL). The combined organic layer was dried over anhydrous sodium sulphate and evaporated *in vacuo* to yield the residue. The crude product was purified by column chromatography using DCM/MeOH = 95:5 as the elution system to obtain 62 mg (78%) of **11** as a pale-yellow oil.

tert-Butyl 4-(8-methoxy-8-oxooctanoyl)piperazine-1-carboxylate (**11**)

R_f = 0.62 (DCM/MeOH = 95:5). **^{1}H NMR** (400 MHz, $CDCl_3$) δ (ppm) = 3.62 (s, 3H), 3.56-3.52 (m, 2H), 3.42-3.39 (m, 4H), 3.37-3.34 (m, 2H), 2.29-2.26 (m, 4H), 1.60-1.57 (m, 4H), 1.43 (s, 9H), 1.32-1.29 (m, 4H). **^{13}C NMR** (100 MHz, $CDCl_3$) δ (ppm) = 174.3, 172.0, 154.7, 80.4, 51.5, 45.5, 41.5, 34.0, 33.3, 29.1, 28.9, 28.5, 25.1, 24.8. **MS** (ESI) 357.20 $[M+H]^+$.

Procedure A for boc-deprotection of aromatic/aliphatic amines

To a solution of boc-protected amine (1 equiv.) in ethyl acetate (30 mL), was added sulphuric acid (3 equiv.) and allowed to stir at room temperature overnight. The compound might not dissolve in ethyl acetate, but upon addition of H_2SO_4, the solution becomes clear. After the completion of reaction, the reaction was quenched with water and extracted with EA (30×3 mL). The combined organic layers were washed with brine and concentrated under reduced pressure, further directly used for the next step in synthesis.

Methyl 8-((4-aminophenyl)amino)-8-oxooctanoate (**9**)

Procedure A was followed using: To **8** (1.78 g, 4.7 mmol, 1 equiv.) in ethyl acetate (30 mL), was added sulphuric acid (0.77 mL, 14.11 mmol, 3 equiv.). The reaction mixture was extracted with EA, washed with brine and concentrated under reduced pressure to obtain 1.30 g (77%) of the product **9** as a brown solid.

R_f = 0.60 (Hex/EA = 1:1). **^{1}H NMR** (400 MHz, $CDCl_3$) δ (ppm) = 7.30 (bs, 1H), 7.26-7.23 (m, 2H), 6.63-6.59 (m, 2H), 3.65 (s, 3H), 2.31-2.25 (m, 4H), 1.70-1.59 (m, 4H), 1.35-1.32 (m, 4H), 1.27-1.22 (m, 2H). **^{13}C NMR** (100 MHz, $CDCl_3$) δ (ppm) = 174.4, 171.2, 143.4, 129.5, 122.2, 115.5, 51.6, 37.5, 34.1, 28.9, 28.9, 25.6, 24.8. **MS** (ESI) 279.10 $[M+H]^+$.

Methyl 8-oxo-8-(piperazin-1-yl)octanoate (**12**)

Procedure A was followed using: To **11** (62 mg, 0.18 mmol, 1 equiv.) in ethyl acetate (30 mL), was added sulphuric acid (0.29 mL, 0.53 mmol, 3 equiv.) to obtain 44 mg (54%) of **12** as a pale yellow oil.

R_f = 0.43 (DCM/MeOH = 9:1 + 0.5% TEA). **^{1}H NMR** (400 MHz, $CDCl_3$) δ (ppm) = 3.65 (s, 3H), 3.61-3.58 (m, 2H), 3.44-3.42 (m, 2H), 2.89-2.82 (m, 4H), 2.25-2.17 (m, 3H), 1.64-1.60 (m, 5H), 1.36-1.32 (m, 5H). **^{13}C NMR** (100 MHz, $CDCl_3$) δ (ppm) = 173.8, 171.6, 60.2, 51.5, 46.2, 34.0, 33.1, 29.1, 28.9, 25.1, 24.8. **MS** (ESI) 257.3 $[M+H]^+$.

Procedure B for 4-substituted 2-chloro-6,7-dimethoxyquinazolines

To a solution of 2,4-dichloro-6,7-dimethoxyquinazoline (1.0 equiv.) in DMF or THF (3.0 mL), corresponding alicyclic amine (2.2 equiv) was added followed by the addition of DIPEA (1.05 equiv). The reaction mixture was stirred at room temperature until TLC showed the consumption of the starting material. The reaction mixture was quenched with water, which was further extracted with EA (20×3 mL). The combined organic phases were washed with 0.5% acetic acid and subsequently with brine, to remove the excess amine. The organic layer was dried over anhydrous Na_2SO_4, concentrated *in vacuo* to yield the crude product, which was purified by flash chromatography using silica gel.

N-(1-Benzylpiperidin-4-yl)-2-chloro-6,7-dimethoxyquinazolin-4-amine (**15a**)

Procedure B was followed using: 2,4-dichloro-6,7-dimethoxyquinazoline (259 mg, 1.0 mmol, 1.0 equiv.), 4-aminol-1-benzylpiperidine (0.448 mL, 2.2 mmol, 2.2 equiv.), DIPEA (0.192 mL, 1.05 mmol, 1.05 equiv.) in 3 mL of DMF. The obtained crude compound was purified by flash chromatography (elution system- DCM/MeOH = 97:3) to yield 243 mg (59%) of **15a** as a yellow crystalline solid.

R_f = 0.38 (DCM/MeOH = 95:5). **^{1}H NMR** (400 MHz, CDCl3) δ (ppm) = 7.30-7.24 (m, 5H), 7.11 (s, 1H), 7.05 (s, 1H), 6.29 (d, *J*= 8.3 Hz, 1H), 4.32-4.23 (m, 1H), 3.91 (s, 3H), 3.89 (s, 3H), 3.49 (s, 2H), 2.89-2.81 (m, 2H), 2.20-2.05 (m, 4H), 1.62-1.52 (m, 2H). **^{13}C NMR** (100 MHz, CDCl3) = 159.4, 156.2, 154.9, 148.9, 147.8, 137.8, 129.2, 128.3, 127.2, 107.0, 106.8, 100.5, 62.9, 56.2, 56.1, 52.3, 48.4, 31.9. **MS** (ESI) 413.2 $[M+H]^+$.

2-Chloro-N-(1-(2-fluorobenzyl)piperidin-4-yl)-6,7-dimethoxyquinazolin-4-amine (**15b**)

Procedure B was followed using: 2,4-dichloro-6,7-dimethoxyquinazoline (259 mg, 1.0 mmol, 1.0 equiv.), 4-aminol-1-(*o*-flouro-benzyl) piperidine (312 mg, 1.5 mmol, 1.5 equiv.), DIPEA (347 µL, 2 mmol, 2 equiv.), K_2CO_3 (1.029 g, 7.46 mmol, 7.46 equiv.) in 10 mL of THF/MeCN. The obtained crude compound was purified by flash chromatography (elution system- DCM/MeOH = 97:3) to yield 327 mg (76%) of **15b** as a white crystalline solid.

R_f = 0.23 (DCM/MeOH = 95:5). **^{1}H NMR** (400 MHz, $CDCl_3$) δ (ppm) = 7.34-7.20 (m, 3H), 7.12-7.01 (m, 3H), 6.57 (bs, 1H), 4.31-4.23 (m, 1H), 3.87 (s, 3H), 3.83 (s, 3H), 3.58 (s, 2H), 2.90-2.88 (m, 2H), 2.24-2.18 (m, 2H), 2.11-2.08 (m, 2H), 1.68-1.60 (m, 2H). **^{13}C NMR** (100 MHz, $CDCl_3$) = 162.5, 160.1, 159.4, 156.1, 148.8, 147.7, 131.5, 128.8, 124.5, 123.7, 115.2, 107.0, 106.6, 100.8, 56.0, 56.0, 55.0, 52.0, 48.6, 31.8. **MS (ESI):** 431.3 $[M+H]^+$.

2-Chloro-N-(1-(2-chlorobenzyl)piperidin-4-yl)-6,7-dimethoxyquinazolin-4-amine (**15c**)

Procedure B was followed using: 2,4-dichloro-6,7-dimethoxyquinazoline (194 mg, 0.75 mmol, 1.5 equiv.), 4-Aminol-1-(*o*-chlorobenzyl)piperidine (112 mg, 0.5 mmol, 1.0 equiv.), K_2CO_3 (510 mg, 3.7 mmol, 7.4 equiv.) in 5 mL of THF. The obtained crude compound was purified by flash chromatography (elution system- DCM/MeOH = 97:3) to yield 120 mg (36%) of **15c** as a yellow solid.

R_f = 0.50 (DCM/MeOH = 95:5)**. ^{1}H NMR** (400 MHz, CDCl3) δ (ppm) = 7.6 (d, *J*= 7.2 Hz, 1H), 7.40-7.37 (m, 1H), 7.30-7.27 (m, 1H), 7.24-7.22 (m, 1H), 7.13 (s, 1H), 6.84 (s, 1H), 5.5 (d, *J* =7.2 Hz, 1H), 4.41-4.33 (m, 1H), 4.01 (s, 3H), 3.97 (s, 3H), 3.81 (s, 2H), 3.08-3.05 (m, 2H), 2.54-2.47 (m, 2H), 2.19-2.16 (m, 2H), 1.87-1.81 (m, 2H). **MS** (ESI) 447.3 $[M+H]^+$.

tert-Butyl 4-((2-chloro-6,7-dimethoxyquinazolin-4-yl)amino)piperidine-1-carboxylate (**17**)

Procedure B was followed using: 2,4-dichloro-6,7-dimethoxyquinazoline (259 mg, 1.0 mmol, 1.0 equiv.), 4-Amino-1-Boc-piperidine (300 mg, 1.5 mmol, 1.5 equiv.), DIPEA (347 µL, 2 mmol, 2 equiv.) in 5 mL of THF. The obtained crude compound was purified by flash chromatography (elution system- DCM/MeOH = 95:5 +1% TEA) to yield 300 mg (71%) of **17** as a yellow amorphous solid.

R_f = (DCM/MeOH = 95:5). **^{1}H NMR** (400 MHz, $CDCl_3$) δ (ppm) = 7.11 (s, 1H), 6.97 (s, 1H), 5.84 (d, *J*= 7.2 Hz, 1H), 4.48-4.39 (m, 1H), 4.21-4.11 (m, 2H), 3.95 (s, 3H), 3.94 (s, 3H), 2.97-2.87 (m, 2H), 2.14-2.11 (m, 2H), 1.56-1.41 (m, 2H), 1.45 (s, 9H). **^{13}C NMR** (100 MHz, $CDCl_3$) = 159.2, 156.1, 155.2, 154.9, 149.3, 148.1, 107.2, 106.8, 100.2, 56.5, 56.4, 48.6, 43.0, 32.2, 28.6. **MS (ESI):** 423.15 $[M+H]^+$.

Procedure for Boc-deprotection of 17

To the solution of **17** (300 mg, 0.710 mmol, 1.0 equiv.) in 2-5 mL methanol, was added the acetyl chloride (1 mL, 14.2 mmol, 20.0 equiv.), with the RBF maintained at 0°C ice bath. The reaction mixture was allowed to stir at room temperature for 12 h. On completion of the reaction, the reaction mixture was concentrated by removal of methanol *in vacuo*. The residue was re-dissolved in DCM, washed with saturated sodium bicarbonate solution to remove the remnant acid. The organic layer was dried with anhydrous Na_2SO_4, concentrated *in vacuo* to yield 222 mg (96%) of crude product **18** as a white amorphous solid which was directly used in the next step.

2-Chloro-6,7-dimethoxy-N-(piperidin-4-yl)quinazolin-4-amine (**18**)

R_f = 0.18 (DCM/MeOH = 95:5 + 0.5% TEA). **^{1}H NMR** (400 MHz, $CDCl_3$) δ (ppm) = 7.26 (bs, 1H), 7.10 (s, 1H), 6.96 (s, 1H), 5.81 (d, *J* = 7.7 Hz, 1H), 4.42-4.34 (m, 1H), 3.97 (s, 3H), 3.93 (s, 3H), 3.17-3.15 (m, 2H), 2.84-2.78 (m, 2H), 2.17-2.14 (m, 2H), 1.61-1.54 (m, 2H). **^{13}C NMR** (100 MHz, $CDCl_3$) = 159.2, 156.3, 155.1, 149.2, 148.2, 107.3, 106.9, 100.2, 56.6, 56.4, 48.5, 45.4, 33.0. **MS (ESI):** 347.3 $[M+H+MeCN]^+$.

Procedure C for reductive amination of aldehydes

To a solution of **18** (1.0 equiv.) in methanol, was added the corresponding benzaldehyde (1.2 equiv.), $Na(CN)BH_3$ (2.0 equiv.) with acetic acid (0.2 equiv.) in catalytic amounts. The reaction was allowed to stir at room temperature overnight. After completion, the reaction solvent was evaporated and the crude product was purified by column chromatography using DCM/methanol as the elution system.

2-Chloro-6,7-dimethoxy-N-(1-(3-methoxybenzyl)piperidin-4-yl)quinazolin-4-amine (**15d**)

Procedure C was followed using: **18** (389 mg, 1.20 mmol, 1.0 equiv.), *p*-methoxybenzaldehyde (290 µL, 2.4 mmol, 2.0 equiv.), $Na(CN)BH_3$ (149 mg, 2.4 mmol, 2.0 equiv.), acetic acid (27 µL, 0.48 mmol, 0.2 equiv.) in 5 mL of methanol. The obtained crude product was purified by column chromatography (DCM/MeOH = 95:5) to yield 132 (29%) of **15d** as a yellow crystalline solid.

R_f = 0.42 (DCM/MeOH = 95:5). **^{1}H NMR** (400 MHz, $CDCl_3$) δ (ppm) = 7.20-7.19 (m, 1H), 7.17-7.16 (m, 1H), 7.06 (s, 1H), 7.03 (s, 1H), 6.82-6.81 (m, 1H), 6.80-6.79 (m, 1H), 6.21 (d, *J*= 8.0 Hz, 1H), 4.31-4.21 (m, 1H), 3.88 (s, 3H), 3.87 (s, 3H), 3.76 (s, 3H), 3.48 (s, 2H), 2.91-2.88 (m, 2H), 2.19-2.04 (m, 4H), 1.73-1.63 (m, 2H). **^{13}C NMR** (100 MHz, $CDCl_3$) = 159.4, 159.0, 156.2, 154.9, 149.0, 148.0, 130.7, 129.0, 113.7, 107.0, 100.5, 62.2, 56.4, 56.2, 55.3, 52.1, 48.2, 31.7. **MS (ESI):** 445.00$[M+2]^+$.

2-Chloro-N-(1-(4-fluorobenzyl) piperidin-4-yl)-6,7-dimethoxyquinazolin-4-amine (**15e**)

Procedure C was followed using: **18** (129 mg, 0.399 mmol, 1.0 equiv.), *p*-flourobenzaldehyde (85 µL, 0.79 mmol, 2.0 equiv.), $Na(CN)BH_3$ (124 mg, 1.7 mmol, 2.0 equiv.), acetic acid (10 µL, 0.16 mmol, 0.4 equiv.) in 5 mL of methanol. The obtained crude product was purified by column chromatography (DCM/MeOH = 95:5) to yield 127 (75%) of **15e** as a pale white crystalline solid.

R_f = 0.36 (DCM/MeOH = 95:5). **^{1}H NMR** (400 MHz, CDCl3) δ (ppm) = 7.25-7.22 (m, 2H), 7.17 (s, 1H), 7.03 (s, 1H), 6.99-6.94 (m, 2H), 6.4 (d, *J* = 7.3 Hz, 1H), 4.32-4.22 (m, 1H), 3.86 (s, 3H), 3.84 (s, 3H), 3.45 (s, 2H), 2.86-2.83 (m, 2H), 2.16-2.04 (m, 4H), 1.68-1.58 (m, 2H). **^{13}C NMR** (100 MHz, CDCl3) δ (ppm) = 163.2, 160.7, 159.4, 156.1, 154.9, 148.9, 147.8, 133.6, 130.6, 115.1, 107.0, 106.7, 100.6, 62.0, 56.1, 56.1, 52.2, 48.6, 31.8. **MS** (ESI) 431.3 $[M+H]^+$.

Procedure for synthesis of 4-substituted 2-chlorothieno[3,2-d]pyrimidines:

To a solution of 2,4-dichlorothieno[3,2-d]pyrimidine (50 mg, 0.25 mmol, 1.0 equiv.) in 5 ml THF, were added the corresponding aliphatic amine (0.075 mL, 0.37 mmol, 1.5 equiv.) and DIPEA (0.065 mL, 0.37 mmol, 1.5 equiv.). The reaction mixture was stirred at 50°C for 4 h, then quenched with water. The aqueous solution was extracted with DCM (3×25 mL), the combined DCM extracts were dried over anhydrous Na_2SO_4. The organic phase was concentrated *in vacuo* to give a crude residue, which was purified by flash chromatography (elution system- DCM/MeOH = 95:5 +1% TEA) to obtain 67 mg (76%) of **20** as a yellow solid.

N-(1-Benzylpiperidin-4-yl)-2-chlorothieno[3,2-d]pyrimidin-4-amine (**20**)

R_f = 0.33 (DCM/MeOH = 95:5)**. ^{1}H NMR** (400 MHz, $CDCl_3$) δ (ppm) = 7.68 (d, *J*= 4.7 Hz, 1H), 7.30-7.21 (m, 6H), 5.19-5.17 (bs, 1H), 4.25-4.16 (m, 1H), 3.52 (s, 2H), 2.87-2.84 (m, 2H), 2.23-2.07 (m, 4H), 1.65-1.56 (m, 2H). **^{13}C NMR** (100 MHz, CDCl3) δ (ppm) = 161.4, 157.7, 157.6, 138.3, 132.3, 129.2, 128.3, 127.2, 124.8, 113.7, 63.1, 52.1, 48.7, 325. **MS** (ESI) 359.1 $[M+H]^+$.

Procedure D for coupling of G9a and HDAC inhibitor precursors:

To the solution of *N*-(1-benzylpiperidin-4-yl)-2-chloro-6,7-dimethoxyquinazolin-4-amine (1.0 equiv.) in IPA (3 ml) in a 2-5 mL microwave vial, was added the respective aliphatic amine

(2.0 equiv.) and HCl in dioxane (2.0 equiv.). The reaction vial was capped and heated in the microwave for 10 min at 160°C. On completion of the reaction, the reaction mixture was concentrated by removal of the solvent *in vacuo*. The residue was redissolved in DCM, washed with saturated sodium bicarbonate solution to remove the remnant acid. The organic layer was dried with anhydrous Na2SO4, concentrated in vacuo to yield the crude product, which was purified by flash chromatography

Isopropyl 8-((4-((4-((1-benzylpiperidin-4-yl)amino)-6,7-dimethoxyquinazolin-2-yl)amino)phenyl)amino)-8-oxooctanoate (**22a**)

Procedure D was followed using: **15a** (372 mg, 0.902 mmol, 1.0 equiv.), **9** (301 mg, 1.08 mmol, 1.2 equiv.), 4 M HCl/Dioxane (0.451 mL, 1.80 mmol, 2.0 equiv.) in 4 mL of IPA. The crude compound was purified by flash chromatography (elution system- DCM/MeOH = 97:3 + 1% TEA) to yield 390 mg (64%) of **22a** as an orange solid.

R_f = 0.38 (DCM/MeOH = 9:1 + 0.5% TEA). **^{1}H NMR** (400 MHz, $CDCl_3$) δ (ppm) = 8.90-8.84 (m, 1H), 7.98-7.92 (m, 1H), 7.60 (s, 1H), 7.45-7.38 (m, 4H), 7.24-7.12 (m, 5H), 6.79-6.70 (m, 1H), 6.59 (s, 1H), 3.99-3.93 (m, 1H), 3.90 (s, 3H), 3.76 (s, 3H), 3.55 (s, 3H), 3.44 (s, 2H), 2.85-2.78 (m, 2H), 2.40-2.37 (m, 2H), 2.22-2.21 (m, 2H), 2.02-1.97 (m, 2H), 1.91-1.84 (m, 4H), 1.67-1.63 (m, 2H), 1.54-1.51 (m, 2H), 1.33-1.27 (m, 4H). **^{13}C NMR** (100 MHz, $CDCl_3$) δ (ppm) = 174.2, 173.3, 172.0, 158.8, 155.3, 151.9, 146.9, 138.6, 137.2, 134.1, 129.4, 128.2, 127.2, 120.9, 120.3, 104.1, 103.2, 100.1, 62.6, 57.1, 56.2, 52.4, 51.4, 49.7, 37.1, 33.9, 30.7, 28.9, 28.8, 25.4, 24.7. **MS** (ESI) 683.40 $[M+H]^+$.

Isopropyl 8-((4-((4-((1-(2-fluorobenzyl)piperidin-4-yl)amino)-6,7-dimethoxyquinazolin-2-yl)amino)phenyl)amino)-8-oxooctanoate (**22b**)

Procedure D was followed using: **15b** (215 mg, 0.50 mmol, 1.0 equiv.), **9** (167 mg, 0.6 mmol, 1.2 equiv.), 4 M HCl/Dioxane (0.25 mL, 1 mmol, 2.0 equiv.) in 3 mL of IPA. The obtained

crude compound was purified by flash chromatography (elution system- DCM/MeOH = 97:3 + 1% TEA) to yield 261 mg (75%) of **22b** as a brown solid.

R_f = 0.4 (DCM/MeOH = 9:1 + 0.5% TEA). **^{1}H NMR** (400 MHz, $CDCl_3$) δ (ppm) = 7.89-7.87 (m, 1H), 7.59-7.57 (m, 2H), 7.42-7.30 (m, 3H), 7.20-7.15 (m, 1H), 7.08-6.95 (m, 3H), 6.85 (s, 1H), 6.59 (s, 1H), 5.82-5.80 (m, 1H), 4.99-4.93 (m, 1H), 4.13-4.10 (m, 1H), 3.84 (s, 3H), 3.83 (s, 3H), 3.80-3.78 (m, 2H), 3.61 (s, 2H), 2.29-2.16 (m, 6H), 2.09-2.06 (m, 2H), 1.66-1.54 (m, 6H), 1.30-1.24 (m, 4H), 1.19 (s, 3H), 1.17 (s, 3H). **MS** (ESI) 701.40 $[M+H]^+$.

Isopropyl 8-((4-((4-((1-(2-chlorobenzyl)piperidin-4-yl)amino)-6,7-dimethoxyquinazolin-2-yl)amino)phenyl)amino)-8-oxooctanoate (**22c**)

Procedure D was followed using: **15c** (186 mg, 0.41 mmol, 1.0 equiv.), **9** (138 mg, 0.50 mmol, 1.2 equiv.), 4 M HCl/Dioxane (0.208 mL, 0.832 mmol, 2.0 equiv.) in 3 mL of IPA. The obtained crude compound was purified by flash chromatography (elution system- DCM/MeOH = 97:3 + 1% TEA) to yield 213 mg (74%) of **22c** as a yellow crystalline solid.

R_f = 0.39 (DCM/MeOH = 9:1 + 0.5% TEA). **^{1}H NMR** (400 MHz, $CDCl_3$) δ (ppm) = 7.66-7.65 (m, 1H), 7.56-7.54 (m, 2H), 7.37-7.35 (m, 3H), 7.25-7.20 (m, 2H), 7.14-7.05 (m, 2H), 6.84-6.81 (m, 2H), 6.82 (s, 1H), 5.53-5.46 (m, 2H), 4.93-4.87 (m, 1H), 4.15-4.07 (m, 1H), 3.79 (s, 3H), 3.78 (s, 3H), 2.84-2.82 (m, 2H), 2.22-2.13 (m, 6H), 2.06-2.02 (m, 2H), 1.62-1.46 (m, 6H), 1.26-2.21 (m, 4H), 1.13 (s, 3H), 1.11 (s, 3H). **^{13}C NMR** (100 MHz, $CDCl_3$) δ (ppm) = 174.3, 173.4, 171.2, 158.7, 154.6, 148.4, 146.1, 137.3, 136.3, 134.3, 131.93, 130.6, 129.4, 128.1, 126.6, 120.8, 119.2, 106.1, 104.5, 101.1, 67.5, 59.3, 56.3, 56.9, 52.7, 48.5, 37.4, 34.6, 34.0, 32.2, 28.8, 25.5, 24.8.

Isopropyl 8-((4-((6,7-dimethoxy-4-((1-(4-methoxybenzyl)piperidin-4-yl)amino)quinazolin-2-yl)amino)phenyl)amino)-8-oxooctanoate (**22d**)

Procedure D was followed using: **15d** (131 mg, 0.30 mmol, 1.0 equiv.), **9** (98 mg, 0.35 mmol, 1.2 equiv.), 4 M HCl/Dioxane (0.15 mL, 0.59 mmol, 2.0 equiv.) in 3 mL of IPA. The obtained crude compound was purified by flash chromatography (elution system- DCM/MeOH = 97:3 + 1% TEA) to yield 166 mg (79%) of **22d** as a brown solid.

R_f = 0.32 (DCM/MeOH = 9:1 + 0.5% TEA). **^{1}H NMR** (400 MHz, $CDCl_3$) δ (ppm) = 7.62-7.56 (m, 3H), 7.42-7.40 (m, 2H), 7.22-7.18 (m, 2H), 6.92-6.82 (m, 4H), 5.48-5.47 (m, 1H), 5.01-4.95 (m, 1H), 4.21-4.11 (m, 1H), 3.90-3.89 (m, 1H), 3.88 (s, 3H), 3.87 (s, 3H), 3.77 (s, 3H), 3.46 (s, 2H), 2.89-2.86 (m, 2H), 2.31-2.09 (m, 9H), 1.73-1.55 (m, 6H), 1.37-1.30 (m, 3H), 1.20 (s, 3H), 1.19 (s, 3H). **^{13}C NMR** (100 MHz, $CDCl_3$) δ (ppm) = 174.3, 173.4, 171.2, 158.8, 158.7, 156.5, 154.7, 148.3, 146.2, 137.3, 132.0, 130.4, 120.8, 119.2, 113.7, 106.1, 104.4, 101.0, 67.5, 62.4, 56.4, 56.0, 55.3, 52.5, 48.6, 46.3, 34.6, 32.3, 28.9, 24.8, 21.9. **MS** (ESI) 713.30 $[M+H]^+$.

Methyl 8-((4-((4-((1-(4-fluorobenzyl)piperidin-4-yl)amino)-6,7-dimethoxyquinazolin-2-yl)amino)phenyl)amino)-8-oxooctanoate (**22e**)

Procedure D was followed using: **15e** (185 mg, 0.43 mmol, 1.0 equiv.), **9** (143 mg, 0.52 mmol, 1.2 equiv.), 4 M HCl/Dioxane (0.215 mL, 0.86 mmol, 2.0 equiv.) in 3 mL of IPA. The obtained crude compound was purified by flash chromatography (elution system- DCM/MeOH = 97:3 + 1% TEA) to yield 167 mg (80%) of **22e** as a yellowish brown solid.

R_f = 0.29 (DCM/MeOH = 9:1 + 0.5% TEA). **^{1}H NMR** (400 MHz, $CDCl_3$) δ (ppm) = 7.64-7.60 (m, 2H), 7.44-7.25 (m, 5H), 7.19-7.05 (bs, 1H), 7.02-6.80 (m, 4H), 5.36-5.34 (bs, 1H), 5.02-4.95 (m, 1H), 4.12-4.10 (m, 1H), 3.91 (s, 3H), 3.90 (s, 3H), 3.48 (s, 2H), 2.89-2.86 (m, 2H), 2.33-2.11 (m, 8H), 1.74-1.58 (m, 6H), 1.39-1.31 (m, 4H), 1.21 (s, 3H), 1.20 (s, 3H). **^{13}C NMR** (100 MHz, $CDCl_3$) δ (ppm) = 173.3, 171.1, 163.2, 160.8, 158.6, 154.7, 148.3, 146.2, 137.2, 134.2, 131.9, 130.5, 120.7, 119.2, 115.1, 106.1, 104.3, 100.9, 67.5, 62.3, 56.4, 56.1, 52.6, 51.6, 48.5, 46.4, 34.7, 32.4, 28.9, 24.9, 25.5, 22.0. **MS** (ESI) 701.30 $[M+H]^+$.

Isopropyl 7-((4-((1-benzylpiperidin-4-yl)amino)-6,7-dimethoxyquinazolin-2-yl)amino)heptanoate (**22f**)

Procedure D was followed using: **15a** (150 mg, 0.364 mmol, 1.0 equiv.), 7-Aminoheptanoicacid methyl ester (85 mg, 0.436 mmol, 1.2 equiv.), 4 M HCl/Dioxane (0.182 mL, 0.728 mmol, 2.0 equiv.) in 4 mL of IPA. The crude compound was purified by flash chromatography (elution system- DCM/MeOH = 97:3 + 1% TEA) to obtain 167 mg (86%) of **22f** as a brown solid.

R_f = 0.27 (DCM/MeOH = 9:1 + 0.5% TEA). **^{1}H NMR** (400 MHz, $CDCl_3$) δ (ppm) = 8.50 (bs, 1H), 7.90 (bs, 1H), 7.74 (bs, 1H), 7.35-7.22 (bs, 5H), 6.79 (bs, 1H), 4.98-4.95 (m, 1H), 4.02 (s, 3H), 3.88 (s, 3H), 3.67-3.65 (m, 1H), 3.63-3.60 (m, 2H), 3.43-3.37 (m, 3H), 3.11-3.05 (m, 2H), 2.29-2.21 (m, 5H), 2.15-2.05 (m, 5H), 1.63-1.55 (m, 5H), 1.40-1.28 (m, 6H). **^{13}C NMR** (100 MHz, CD_3OD) δ (ppm) = 174.1, 173.3, 159.1, 155.7, 153.2, 147.1, 135.6, 129.5, 128.4, 127.6, 105.2, 102.5, 98.2, 67.5, 57.6, 57.6, 53.9, 52.3, 42.2, 34.6, 30.5, 29.4, 28.9, 26.7, 24.9. **MS** (ESI) 536.25 $[M+H]^+$.

Isopropyl 8-(4-(4-((1-benzylpiperidin-4-yl)amino)-6,7-dimethoxyquinazolin-2-yl)piperazin-1-yl)-8-oxooctanoate (**22g**)

Procedure D was followed using: **15a** (463 mg, 1.125 mmol, 1.2 equiv.), **12** (240 mg, 0.937 mmol, 1.0 equiv.), 4 M HCl/Dioxane (0.468 mL, 1.87 mmol, 2.0 equiv.) in 4 mL of IPA. The obtained crude compound was purified by flash chromatography (elution system- DCM/MeOH = 97:3 + 150 µL NH_4OH) to yield 163 mg (27%) of **22g** as an orange solid.

R_f = 0.38 (DCM/MeOH = 9:1 + 0.005% NH_4OH). **^{1}H NMR** (400 MHz, $CDCl_3$), δ (ppm) = 7.33-7.25 (m, 5H), 6.90 (s, 1H), 6.74 (s, 1H), 5.16 (d, *J* = 7.7 Hz, 1H), 4.14-4.10 (m, 2H), 3.94 (s, 3H), 3.92 (s, 3H), 3.87-3.78 (m, 4H), 3.71-3.68 (m, 2H), 3.55 (s, 2H), 3.53-3.51 (m, 2H) 2.93-2.90 (m, 2H), 2.38-2.34 (m, 2H), 2.30-2.17 (m, 4H), 2.13-2.11 (m, 2H), 1.68-1.60 (m, 6H), 1.38-1.35 (m, 4H), 1.26-1.20 (m, 6H). **^{13}C NMR** (100 MHz, $CDCl_3$), δ (ppm) = 173.4,

171.8, 158.7, 158.4, 154.6, 149.1, 145.9, 138.4, 129.3, 128.4, 127.2, 106.2, 103.5, 100.8, 67.5, 63.2, 56.4, 56.1, 52.6, 48.4, 45.8, 44.5, 41.7, 34.7, 33.5, 32.3, 29.3, 29.0, 25.3, 22.0. **MS** (ESI) 661.45 $[M+H]^+$.

Isopropyl 8-((4-((4-((1-benzylpiperidin-4-yl)amino)thieno[3,2-d]pyrimidin-2-yl)amino)phenyl)amino)-8-oxooctanoate (**22h**)

Procedure D was followed using: **20** (372 mg, 0.902 mmol, 1.0 equiv.), **9** (301 mg, 1.08 mmol, 1.2 equiv.), 4 M HCl/Dioxane (0.451 mL, 1.80 mmol, 2.0 equiv.) in 4 mL of IPA. The obtained crude compound was purified by flash chromatography (elution system- DCM/MeOH = 97:3 + 1% TEA) to yield 142 mg (81%) of **22h** as a yellow solid.

R_f = 0.31 (DCM/MeOH = 9:1 + 0.5% TEA). **^{1}H NMR** (400 MHz, $CDCl_3$) δ (ppm) = 7.62 (bs, 1H), 7.51 (d, *J* = 8.7 Hz, 2H), 7.52 (d, *J* = 5.5 Hz, 1H), 7.4 (d, *J* = 8.7 Hz, 2H), 7.28-7.21 (m, 6H), 7.11 (d, *J* = 5.5 Hz, 1H), 5.00-4.93 (m, 1H), 4.82 (bs, 1H), 4.17-4.06 (m, 1H), 3.49 (s, 2H), 2.86-2.83 (m, 2H), 2.28-2.05 (m, 8H), 1.71-1.64 (m, 2H), 1.61-1.53 (m, 4H), 1.34-1.26 (m, 4H), 1.19 (s, 3H), 1.17 (s, 3H). **^{13}C NMR** (100 MHz, $CDCl_3$) δ (ppm) = 173.4, 171.3, 161.3, 158.4, 157.0, 138.5, 137.1, 132.2, 130.8, 129.2, 128.3, 127.1, 124.3, 120.8, 119.4, 107.6, 67.5, 63.0, 52.5, 48.6, 37.5, 34.7, 32.4, 28.9, 25.5, 24.9, 21.9. **MS** (ESI) 629.30 $[M+H]^+$.

Procedure E for hydrolysis of isopropyl/methyl esters

To a solution of the methyl/*iso*propyl ester (1.0 equiv.), was added LiOH (10 equiv.) dissolved in in THF/Water (2:1). The reaction was stirred at 60^0C for 8-10 h (specified for each derivative) and was monitored by TLC and/or LC/MS. Upon completion (or near completion) of the reaction, the solvent mixture was evaporated under reduced pressure to yield a solid residue, which was re-dissolved in 10-15 mL of distilled water. The aqueous solution was extracted with ether (2×20 mL) to ensure the removal of traces of the unreacted ester, while still retaining the ionized acid in the aqueous phase. The aqueous phase was neutralized by 1M HCl, resulting in the formation of maximum amount of precipitate (in some cases) between pH

5.5-6.5; the solid was filtered and the precipitate was dried under the vacuum pump. In the cases where there was no precipitate formation during HCl neutralization, the pH was adjusted to 8-9 using saturated sodium bicarbonate solution. The aqueous phase was then extracted with ethyl acetate (3×30 mL), further washed with brine solution. The combined organic extract was dried over anhydrous sodium sulphate and concentrated under reduced pressure to give the crude acid, which was used in the further steps without further purification.

8-((4-((4-((1-Benzylpiperidin-4-yl)amino)-6,7-dimethoxyquinazolin-2-yl)amino)phenyl)amino)-8-oxooctanoic acid (**23a**)

Procedure E was followed using: **22a** (390 mg, 0.596 mmol, 1.0 equiv.), LiOH (143 mg, 5.96 mmol, 10 equiv.) in THF/water (10 mL:5 mL) for 8h. The aqueous phase was then extracted with ethyl acetate (3×30 mL), further washed with brine solution. The combined organic extract was dried over anhydrous sodium sulphate and concentrated under reduced pressure to yield 215 mg (57%) of **23a** as a brown amorphous solid.

R_f = 0.18 (DCM/MeOH = 9:1 + 0.5% TEA). **^{1}H NMR** (400 MHz, $CDCl_3$/CD_3OD) δ (ppm) = 7.63-7.59 (m, 3H), 7.45-7.37 (m, 7H), 7.05 (s, 1H), 4.40-4.32 (m, 1H), 4.26 (s, 2H), 3.96 (s, 3H), 3.94 (s, 3H), 3.46-3.43 (m, 2H), 3.05-2.97 (m, 2H), 2.35-2.32 (m, 4H), 2.27-2.22 (m, 2H), 2.10-2.07 (m, 2H), 1.72-1.66 (m, 2H), 1.62-1.55 (m, 2H), 1.39-1.31 (m, 4H). **MS** (ESI) 641.30 $[M+H]^+$.

8-((4-((4-((1-(2-Fluorobenzyl)piperidin-4-yl)amino)-6,7-dimethoxyquinazolin-2-yl)amino)phenyl)amino)-8-oxooctanoic acid (**23b**)

Procedure E was followed using: **22b** (261 mg, 0.372 mmol, 1.0 equiv.), LiOH (179 mg, 7.45 mmol, 10 equiv.) in THF/water (10 mL:5 mL) for 6 h. The aqueous phase was then extracted with ethyl acetate (3×30 mL), further washed with brine solution. The combined organic

extract was dried over anhydrous sodium sulphate and concentrated under reduced pressure to yield 156 mg (64%) of **23b** as a dark brown solid.

R_f = 0.15 (DCM/MeOH = 9:1 + 0.5% TEA). **^{1}H NMR** (400 MHz, CD_3OD) δ (ppm) = 7.70-7.24 (m, 9H), 6.96 (s, 1H), 4.36 (s, 2H), 4.35-4.25 (m, 1H), 3.93 (s, 3H), 3.91 (s, 3H), 3.56-3.53 (m, 2H), 3.11-3.05 (m, 2H), 2.44-2.40 (m, 2H), 2.29-2.26 (m, 4H), 2.15-2.04 (m, 2H), 1.77-1.69 (m, 2H), 1.66-1.58 (m, 2H), 1.45-1.36 (m, 4H). **^{13}C NMR** (100 MHz, CD_3OD) δ (ppm) = 177.8, 174.6, 164.3, 161.9, 160.9, 157.8, 152.7, 149.3, 137.7, 137.1, 134.7, 133.7, 126.2, 125.1, 122.2, 118.8, 117.1, 105.3, 104.2, 99.8, 57.3, 57.0, 54.6, 52.8, 49.3, 37.8, 35.1, 30.0, 29.4, 26.7, 26.0. **MS** (ESI) 659.25 $[M+H]^+$.

7-((4-((1-Benzylpiperidin-4-yl)amino)-6,7-dimethoxyquinazolin-2-yl)amino)heptanoic acid (**23f**)

Procedure E was followed using: **22f** (195 mg, 0.36 mmol, 1.0 equiv.), LiOH (82 mg, 3.6 mmol, 10 equiv.) in THF/water (10 mL:5 mL) for 8h. The aqueous phase was then extracted with ethyl acetate (3×30 mL), further washed with brine solution. The combined organic extract was dried over anhydrous sodium sulphate and concentrated under reduced pressure to yield 135 mg (71%) of **23f** as a pale white solid.

R_f = 0.19 (DCM/MeOH = 9:1 + 0.5% TEA). **^{1}H NMR** (400 MHz, $(CD_3)_2SO$) δ (ppm) = 7.40 (s, 1H), 7.35-7.30 (m, 4H), 7.27-7.23 (m, 1H), 7.16 (bs, 1H), 6.65 (s, 1H), 6.16 (bs, 1H), 4.17-4.08 (m, 1H), 3.93 (bs, 1H), 3.80 (s, 3H), 3.79 (s, 3H), 3.49 (s, 2H), 3.25-3.20 (m, 2H), 2.88-2.85 (m, 2H), 2.18-2.15 (m, 2H), 2.06-2.00 (m, 2H), 1.91-1.88 (m, 2H), 1.65-1.61 (m, 2H), 1.51-1.48 (m, 4H), 1.31-1.27 (m, 4H). **^{13}C NMR** (100 MHz, $(CD_3)_2SO$) δ (ppm) = 174.7, 158.8, 158.3, 153.7, 148.6, 144.2, 138.6, 128.7, 128.1, 126.8, 103.5, 62.1, 56.0, 55.2, 54.8, 52.5, 40.7, 34.1, 31.7, 28.5, 26.4, 24.7. **MS** (ESI) 522.30 $[M+H]^+$.

8-(4-(4-((1-Benzylpiperidin-4-yl)amino)-6,7-dimethoxyquinazolin-2-yl)piperazin-1-yl)-8-oxooctanoic acid (**23g**)

Procedure E was followed using: **22g** (198 mg, 0.299 mmol, 1.0 equiv.), LiOH (72 mg, 2.99 mmol, 10 equiv.) in THF/water (10 mL:5 mL) for 6h. The aqueous phase was then extracted with ethyl acetate (3×30 mL), further washed with brine solution. The combined organic extract was dried over anhydrous sodium sulphate and concentrated under reduced pressure to yield 180 mg (97%) of **23g** as a white solid.

R_f = 0.22 (DCM/MeOH = 9:1 + 0.004% NH_4OH). **^{1}H NMR** (400 MHz, CD_3OD), δ (ppm) = 7.40 (s, 1H), 7.33-7.26 (m, 5H), 6.86 (s, 1H), 4.14-4.08 (m, 1H), 3.89 (s, 3H), 3.88 (s, 3H), 3.84-3.81 (m, 2H), 3.78-3.75 (m, 2H), 3.65-3.62 (m, 2H), 3.61-3.58 (m, 2H), 3.54 (s, 2H), 2.97-2.94 (m, 2H), 2.44-2.40 (m, 2H), 2.20-2.15 (m, 4H), 2.07-2.04 (m, 2H), 1.75-1.69 (m, 2H), 1.66-1.59 (m, 4H), 1.39-1.37 (m, 4H). **^{13}C NMR** (100 MHz, CD_3OD), δ (ppm) = 174.4, 172.9, 169.2, 160.2, 157.6, 156.4, 147.9, 136.1, 131.3, 129.6, 129.2, 104.8, 104.3, 104.1, 63.1, 56.9, 56.5, 53.3, 46.5, 45.7, 45.3, 42.5, 40.1, 34.0, 31.3, 30.2, 26.9, 26.4. **MS** (ESI) 619.40 $[M+H]^+$.

8-((4-((4-((1-Benzylpiperidin-4-yl)amino)thieno[3,2-d]pyrimidin-2-yl)amino)phenyl)amino)-8-oxooctanoic acid (**23h**)

Procedure E was followed using: **22h** (390 mg, 0.596 mmol, 1.0 equiv.), LiOH (143 mg, 5.96 mmol, 10 equiv.) in THF/water (10 mL:5 mL) for 8h. The aqueous phase was then extracted with ethyl acetate (3×30 mL), further washed with brine solution. The combined organic extract was dried over anhydrous sodium sulphate and concentrated under reduced pressure to yield 43 mg (33%) of **23h** as a brown solid.

R_f = 0.24 (DCM/MeOH = 9:1 + 0.5% TEA). **^{1}H NMR** (400 MHz, $(CD_3)_2SO$, δ (ppm) = 9.66 (bs, 1H), 8.84 (bs, 1H), 7.92 (d, *J* = 5.2 Hz, 1H), 7.71-7.69 (m, 2H), 7.45-7.43 (m, 3H), 7.34-7.33 (m, 4H), 7.27-7.24 (m, 1H), 7.1 (d, *J* = 5.1 Hz, 1H), 4.14-4.04 (m, 1H), 3.55 (bs, 1H), 3.52 (s, 2H), 2.93-2.89 (m, 2H), 2.29-2.25 (m, 2H), 2.22-2.18 (m, 2H), 2.11-2.06 (m, 2H), 1.95-1.92 (m, 2H), 1.67-1.48 (m, 6H), 1.35-2.27 (m, 4H). **^{13}C NMR** (100 MHz, $(CD_3)_2SO$), δ

(ppm) = 174.4, 170.6, 161.0, 158.1, 156.4, 137.2, 132.4, 132.3, 128.8, 128.1, 126.9, 123.3, 119.4, 118.3, 106.6, 62.1, 52.5, 48.0, 36.2, 33.6, 31.4, 28.4, 28.3, 25.1, 24.4. **MS** (ESI) 587.20 $[M+H]^+$.

Procedure F for amide protection by tetrhydropyranhydroxylamine (THP)

To a solution of the respective acid (1.0 equiv.) in 5 mL DMF, was added the coupling agent HATU (1.2 equiv.) in triethylamine (3 equiv.). This was followed by the addition of the protecting agent tetrahydropyran hydroxylamine (1.1 equiv.) and the reaction was stirred overnight at room temperature. The reaction was monitored by TLC for the complete conversion of the starting material. The reaction was quenched with water and extracted with EA (30×3 mL). The combined organic layers were further washed with brine and dried over anhydrous sodium sulphate. The organic layer was concentrated *in vacuo* to yield the crude residue, which was purified by flash chromatography.

N1-(4-((4-((1-Benzylpiperidin-4-yl)amino)-6,7-dimethoxyquinazolin-2-yl)amino)phenyl)-N8-((tetrahydro-2H-pyran-2-yl)oxy)octanediamide (**24a**)

Procedure F was followed using: **23a** (215 mg, 0.36 mmol, 1.0 equiv.), HATU (153 mg, 0.40 mmmol, 1.2 equiv.), triethylamine (0.233 µL, 1.67 mmol, 5.0 equiv.), tetrahydropyran hydroxylamine (43 mg, 0.37 mmol, 1.1 equiv.) in 4 mL DMF. The crude residue was purified using flash chromatography (elution system- DCM/MeOH = 95:5 + 0.5% TEA) to obtain 138 mg (56%) of **24a** as a yellow solid.

R_f = 0.26 (DCM/MeOH = 9:1 + 0.5% TEA). **^{1}H NMR** (400 MHz, $CDCl_3$) δ (ppm) = 8.14 (bs, 1H), 7.56-7.47 (m, 4H), 7.35-7.21 (m, 5H), 7.12 (bs, 1H), 6.79 (bs, 1H), 6.39 (bs, 1H), 4.99-4.92 (m, 1H), 4.19-4.07 (m, 1H), 3.97 (s, 3H), 3.96-3.92 (m, 1H), 3.91 (s, 3H), 3.59 (m, 2H), 3.57-3.54 (m, 1H), 2.96-2.90 (m, 2H), 2.37-2.33 (m, 2H), 2.25-2.18 (m, 2H), 2.11-2.06 (m, 4H), 1.84-1.54 (m, 13H), 1.40-1.34 (m, 5H). **^{13}C NMR** (100 MHz, $CDCl_3$) δ (ppm) = 191.6, 181.6, 172.0, 168.0, 158.8, 155.3, 154.2, 148.4, 146.9, 135.7, 133.2, 129.5, 128.4, 127.5,

121.1, 120.1, 112.3, 103.8, 103.2, 102.4, 62.7, 56.9, 56.4, 52.5, 49.2, 37.3, 31.4, 28.6, 28.5, 28.2, 25.5, 25.1, 18.7. **MS** (ESI) 740.40 $[M+H]^+$.

N1-(4-((4-((1-(2-Fluorobenzyl)piperidin-4-yl)amino)-6,7-dimethoxyquinazolin-2-yl)amino)phenyl)-N8-((tetrahydro-2H-pyran-2-yl)oxy)octanediamide (**24b**)

Procedure F was followed using: **23b** (156 mg, 0.24 mmol, 1.0 equiv.), HATU (108 mg, 0.28 mmmol, 1.2 equiv.), triethylamine (0.166 µL, 1.19 mmol, 5.0 equiv.), tetrahydropyran hydroxylamine (56 mg, 0.47 mmol, 1.1 equiv.) in 4 mL DMF. The crude residue was purified using flash chromatography (elution system- DCM/MeOH = 95:5 + 0.5% TEA) to yield 153 mg (85%) of **24b** as a brown solid.

R_f = 0.39 (DCM/MeOH = 9:1 + 0.5% TEA). **^{1}H NMR** (400 MHz, $CDCl_3$) δ (ppm) = 8.23 (bs, 1H), 7.59-7.57 (m, 2H), 7.41-7.39 (m, 2H), 7.33-7.29 (m, 1H), 7.18-7.14 (m, 1H), 7.05-7.01 (m, 1H), 6.97-6.95 (m, 1H), 6.93 (s, 1H), 6.84 (s, 1H), 5.77 (d, *J* = 7.5 Hz, 1H), 5.53-5.35 (m, 1H), 4.91 (bs, 1H), 4.11 (bs, 1H), 3.96 (bs, 1H), 3.86 (s, 3H), 3.84 (s, 3H), 3.58-3.56 (m, 1H), 3.53 (s, 2H), 3.37 (s, 1H), 2.89-2.87 (m, 2H), 2.21-2.16 (m, 4H), 2.06-1.97 (m, 4H), 1.70-1.48 (m, 11H), 1.21-1.18 (m, 5H). **^{13}C NMR** (100 MHz, CD_3OD) δ (ppm) = 172.1, 170.9, 162.6, 160.2, 158.8, 156.3, 154. 7, 147.9, 146.3, 137.3, 132.1, 131.7, 128.9, 123.9, 121.3, 119.2, 115.3, 105.6, 104.5, 102.3, 101.5, 63.1, 62.4, 56.4, 56.0, 52.5, 50.1, 37.0, 33.0, 31.9, 28.6, 28.1, 25.4, 25.0, 18.6. **MS** (ESI) 758.25 $[M+H]^+$.

N1-(4-((4-((1-(2-Chlorobenzyl)piperidin-4-yl)amino)-6,7-dimethoxyquinazolin-2-yl)amino)phenyl)-N8-((tetrahydro-2H-pyran-2-yl)oxy)octanediamide (**24c**)

Procedure F was followed using: **23c** (198 mg, 0.29 mmol, 1.0 equiv.), HATU (133 mg, 0.35 mmmol, 1.2 equiv.), triethylamine (0.118 µL, 1.47 mmol, 5.0 equiv.), tetrahydropyran hydroxylamine (69 mg, 0.59 mmol, 1.1 equiv.) in 4 mL DMF. The crude residue was purified

using flash chromatography (elution system- DCM/MeOH = 95:5 + 0.5% TEA) to yield 212 mg (93%) of **24c** as a yellow solid.

R_f = 0.30 (DCM/MeOH = 9:1 + 0.5% TEA). **^{1}H NMR** (400 MHz, $CDCl_3$) δ (ppm) = 8.06 (bs, 1H), 7.60-7.55 (m, 2H), 7.45-7.43 (m, 3H), 7.31-7.28 (m, 1H), 7.21-7.11 (m, 2H), 6.94 (s, 1H), 6.82 (s, 1H), 5.88 (bs, 1H), 5.00-4.94 (m, 1H), 4.19-4.07 (m, 1H), 4.05-3.94 (m, 1H), 3.90 (s, 3H), 3.88 (s, 3H), 3.63-3.62 (m, 1H), 3.60 (s, 2H), 2.94-2.86 (m, 4H), 2.31-2.03 (m, 7H), 1.81-1.52 (m, 11H), 1.37-1.19 (m, 6H). **^{13}C NMR** (100 MHz, $CDCl_3$) δ (ppm) = 172.1, 171.0, 158.8, 155.3, 155.1, 146.6, 146.5, 136.6, 136.17, 134.4, 132.6, 130.8, 129.5, 128.3, 126.7, 121.2, 119.7, 104.6, 104.1, 102.4, 101.6, 62.5, 59.3, 56.5, 56.2, 53.5, 52.7, 49.1, 37.2, 32.1, 28.6, 28.2, 25.3, 25.1. **MS** (ESI) 775.30 $[M+H]^+$.

N1-(4-((6,7-Dimethoxy-4-((1-(4-methoxybenzyl)piperidin-4-yl)amino)quinazolin-2-yl)amino)phenyl)-N8-((tetrahydro-2H-pyran-2-yl)oxy)octanediamide (**24d**)

Procedure F was followed using: **23d** (145 mg, 0.22 mmol, 1.0 equiv.), HATU (98 mg, 0.26 mmmol, 1.2 equiv.), triethylamine (0.150 µL, 1.01 mmol, 5.0 equiv.), tetrahydropyran hydroxylamine (50 mg, 0.43 mmol, 1.1 equiv.) in 4 mL DMF. The crude residue was purified using flash chromatography (elution system- DCM/MeOH = 95:5 + 0.5% TEA) to yield 149 mg (89%) of **24d** as a yellow crystalline solid.

R_f = 0.28 (DCM/MeOH = 9:1 + 0.5% TEA). **^{1}H NMR** (400 MHz, $CDCl_3$) δ (ppm) = 8.00 (bs, 1H), 7.8 (bs, 1H), 7.6 (d, *J*= 8.4 Hz, 2H), 7.45 (d, *J*= 9.8 Hz, 2H), 7.24 (d, *J*= 8.4 Hz, 2H), 6.91-6.90 (m, 1H), 6.86-6.83 (m, 3H), 5.74 (bs, 1H), 4.96 (bs, 1H), 4.20-4.11 (m, 1H), 4.05-3.95 (m, 1H), 3.92 (s, 3H), 3.91 (s, 3H), 3.77 (s, 3H), 3.63-3.57 (m, 1H), 3.54 (s, 2H), 2.93-2.89 (m, 4H), 2.32-2.22 (m, 4H), 2.11-2.03 (m, 3H), 1.79-1.73 (m, 3H), 1.68-1.50 (m, 8H), 1.32-1.25 (m, 5H). **^{13}C NMR** (100 MHz, $CDCl_3$) δ (ppm) = 171.9, 170.8, 159.1, 158.8, 155.7, 155.0, 147.0, 146.6, 136.9, 132.4, 130.7, 121.1, 119.6, 113.8, 105.2, 104.3, 102.5, 101.4,

62.6, 62.1, 56.5, 56.2, 55.4, 52.4, 48.7, 37.2, 31.7, 28.6, 28.5, 28.2, 25.5, 25.4, 25.1, 18.7. **MS** (ESI) 770.35 $[M+H]^+$, 793.30 $[M+Na]^+$.

N1-(4-((4-((1-(4-Fluorobenzyl)piperidin-4-yl)amino)-6,7-dimethoxyquinazolin-2-yl)amino)phenyl)-N8-((tetrahydro-2H-pyran-2-yl)oxy)octanediamide (**24e**)

Procedure F was followed using **23e** (155 mg, 0.24 mmol, 1.0 equiv.), HATU (107 mg, 0.28 mmmol, 1.2 equiv.), triethylamine (0.163 µL, 1.17 mmol, 5.0 equiv.), tetrahydropyran hydroxylamine (55 mg, 0.47 mmol, 1.1 equiv.) in 4 mL DMF. The crude residue was purified using flash chromatography (elution system- DCM/MeOH = 95:5 + 0.5% TEA) to obtain 155 mg (86%) of **24e** as a brown solid.

R_f = 0.25 (DCM/MeOH = 9:1 + 0.5% TEA). **^{1}H NMR** (400 MHz, $CDCl_3$) δ (ppm) = 7.90 (bs, 1H) 7.57-7.53 (m, 2H), 7.38-7.34 (m, 2H), 7.23-7.17 (m, 3H), 6.93-6.88 (m, 2H), 6.82-6.78 (m, 2H), 5.57-5.55 (m, 1H), 4.91-4.87 (m, 1H), 4.13-4.02 (m, 1H), 4.02-3.90 (m, 1H), 3.85 (s, 3H), 3.83 (s, 3H), 3.82-3.72 (m, 1H), 3.55 (m, 1H), 3.42 (s, 2H), 2.95-2.83 (m, 3H), 2.29-1.92 (m, 8H), 1.70-1.39 (m, 11H), 1.25-1.17 (m, 4H). **^{13}C NMR** (100 MHz, $CDCl_3$) δ (ppm) = 172.1, 170.9, 163.2, 160.8, 158.7, 155.8, 154.9, 146.4, 137.0, 134.0, 132.1, 130.5, 121.3, 120.2, 119.3, 115.1, 105.7, 105.3, 104.2, 101.2, 62.5, 61.9, 56.4, 56.2, 52.5, 48.8, 48.7, 37.3, 34.6, 33.1, 31.9, 28.8, 25.3, 25.0, 21.8, 18.8. **MS** (ESI) 758.30 $[M+H]^+$.

7-((4-((1-Benzylpiperidin-4-yl)amino)-6,7-dimethoxyquinazolin-2-yl)amino)-N-((tetrahydro-2H-pyran-2-yl)oxy)heptanamide (**24f**)

Procedure F was followed using: **23f** (110 mg, 0.21 mmol, 1.0 equiv.), HATU (96 mg, 0.25 mmmol, 1.2 equiv.), triethylamine (0.146 µL, 1.05 mmol, 5.0 equiv.), tetrahydropyran hydroxylamine (27 mg, 0.23 mmol, 1.1 equiv.) in 4 mL DMF. The crude residue was purified using flash chromatography (elution system- DCM/MeOH = 95:5 + 0.5% TEA) to yield 78 mg (60%) of **24f** as a brown solid.

R_f = 0.25 (DCM/MeOH = 9:1 + 0.5% TEA). **^{1}H NMR** (400 MHz, $(CD_3)_2SO$) δ (ppm) = 7.41 (s, 1H), 7.33-7.30 (m, 4H), 7.27-7.24 (m, 1H), 6.66 (s, 1H), 6.15 (bs, 1H), 4.79 (bs, 1H), 4.13-4.07 (m, 1H), 3.93-3.88 (m, 1H), 3.80 (s, 3H), 3.79 (s, 3H), 3.50 (s, 2H), 3.48-3.45 (m, 1H), 3.26-3.20 (m, 4H), 2.88-2.86 (m, 2H), 2.06-1.96 (m, 4H), 1.92-1.89 (m, 2H), 1.66-1.61 (m, 5H), 1.53-1.46 (m, 7H), 1.32-1.23 (m, 4H). **^{13}C NMR** (100 MHz, $(CD_3)_2SO$) δ (ppm) = 169.1, 158.6, 158.3, 153.7, 148.1, 144.3, 138.6, 128.7, 128.1, 126.8, 103.5, 103.4, 100.8, 62.1, 61.3, 56.1, 55.3, 52.5, 40.7, 32.2, 31.6, 29.4, 28.4, 27.8, 26.4, 25.0, 24.6, 18.3. **MS** (ESI) 621.40 $[M+H]^+$.

8-(4-(4-((1-Benzylpiperidin-4-yl)amino)-6,7-dimethoxyquinazolin-2-yl)piperazin-1-yl)-8-oxo-N-((tetrahydro-2H-pyran-2-yl)oxy)octanamide (**24g**)

Procedure F was followed using: **23g** (180 mg, 0.307 mmol, 1.0 equiv.), HATU (140 mg, 0.368 mmmol, 1.2 equiv.), triethylamine (0.213 µL, 1.535 mmol, 5.0 equiv.), tetrahydropyran hydroxylamine (40 mg, 0.338 mmol, 1.1 equiv.) in 4 mL DMF. The crude residue was purified using flash chromatography (elution system- DCM/MeOH = 90:10 + 0.2% NH_4OH) to yield 112 mg (54%) of **24g** as a yellow crystalline solid.

R_f = 0.33 (DCM/MeOH = 9:1 + 0.004% NH_4OH). **^{1}H NMR** (400 MHz, $CDCl_3$), δ (ppm) = 7.34-7.23 (m, 5H), 6.91 (s, 1H), 6.84 (s, 1H), 5.52 (bs, 1H), 4.93 (bs, 1H), 4.17-4.10 (m, 1H), 4.00-3.94 (m, 1H), 3.94 (s, 3H), 3.91 (s, 3H), 3.85-3.78 (m, 4H), 3.71-3.60 (m, 3H), 3.58 (s, 2H), 3.56-3.54 (m, 2H), 2.98-2.86 (m, 3H), 2.38-2.34 (m, 2H), 2.29-2.22 (m, 2H), 2.12-2.09 (m, 3H), 1.79-1.73 (m, 3H), 1.70-1.58 (m, 7H), 1.55-1.52 (m, 2H), 1.35-1.24 (m, 5H). **^{13}C NMR** (100 MHz, $CDCl_3$), δ (ppm) = 172.0, 170.7, 158.5, 158.1, 154.7, 147.9, 146.1, 137.8, 129.4, 128.4, 127.4, 105.6, 103.4, 102.4, 101.2, 63.1, 62.5, 56.4, 56.1, 53.5, 52.6, 48.4, 45.7, 44.5, 44.2, 41.7, 33.2, 32.0, 28.8, 28.1, 25.1, 18.7. **MS** (ESI) 718.50 $[M+H]^+$.

8-((4-((4-((1-Benzylpiperidin-4-yl)amino)thieno[3,2-d]pyrimidin-2-yl)amino)phenyl)amino)-8-oxooctanoic acid (**24h**)

Procedure F was followed using: **23h** (40 mg, 0.068 mmol, 1.0 equiv.), HATU (31 mg, 0.81 mmmol, 1.2 equiv.), triethylamine (0.050 µL, 0.34 mmol, 5.0 equiv.), tetrahydropyran hydroxylamine (8.7 mg, 0.075 mmol, 1.1 equiv.) in 4 mL DMF. The crude residue was purified using flash chromatography (elution system- DCM/MeOH = 90:10 + 0.002% NH_4OH) to yield 34 mg (71%) of **24h** as a yellow solid.

R_f = 0.29 (DCM/MeOH = 9:1 + 0.5% TEA). **^{1}H NMR** (400 MHz, $CDCl_3$/CD_3OD), δ (ppm) = 7.76 (d, *J* = 5.5 Hz, 1H), 7.63-7.61 (m, 2H), 7.48-7.45 (m, 2H), 7.37-7.26 (m, 5H), 7.08 (d, *J* = 5.5 Hz, 1H), 4.88 (bs, 1H), 4.20-4.10 (m, 1H), 4.01-3.96 (m, 1H), 3.60 (s, 1H), 3.56 (s, 2H), 3.32-3.30 (m, 2H), 2.99-2.96 (m, 2H), 2.39-2.34 (m, 2H), 2.22-2.11 (m, 6H), 2.08-2.04 (m, 2H), 1.83-1.77 (m, 2H), 1.74-1.71 (m, 4H), 1.68-1.61 (m, 4H), 1.58-1.52 (m, 2H), 1.43-1.39 (m, 4H). **^{13}C NMR** (100 MHz, $CDCl_3$ / CD_3OD), δ (ppm) = 174.3, 172.7, 161.7, 159.8, 158.4, 138.8, 138.4, 133.7, 132.9, 130.8, 129.3, 128.5, 124.0, 121.8, 120.8, 108.9, 103.2, 64.1, 63.0, 53.9, 37.8, 33.7, 32.4, 30.7, 29.9, 29.0, 26.8, 26.5, 26.2, 19.4. **MS** (ESI) 686.30 [M+H]+.

General Procedure G for tetrahydropyranol deprotection

The respective THP-protected ester (1.0 equiv.) was dissolved in THF/Dioxane/DCM, depending on the solubility. To this, 4M HCl/Dioxane (3 equiv.) was added and the reaction mixture was stirred at ambient temperature under nitrogen atmosphere for 12 h. On completion, the solvent was evaporated *in vacuo* resulting in a crude solid. The solid was washed with water, DCM and other organic solvents (specific to the derivative) to remove the impurities, resulting in the pure hydroxamic acid derivative.

N1-(4-((4-((1-Benzylpiperidin-4-yl)amino)-6,7-dimethoxyquinazolin-2-yl)amino)phenyl)-N8-hydroxyoctanediamide hydrochloride **(25a)**

Procedure G was following using **24a** (23 mg, 0.27 mmol, 1.0 equiv.), 4M HCl/Dioxane (0.1 mL, 0.093 mmol, 3 equiv.) in 5 mL THF. The crude product was washed with DCM, further with DCM + 1 % MeOH to yield 14 mg (68%) of **25a** residue as a white amorphous solid.

R_f = 0.16 (DCM/MeOH = 9:1 + 0.5% TEA). **^{1}H NMR** (400 MHz, CD_3OD) δ (ppm) = 7.73 (s, 1H), 7.64-7.60 (m, 4H), 7.52-7.50 (m, 3H), 7.45-7.43 (m, 2H), 7.02 (s, 1H), 4.40 (s, 2H), 4.37-4.30 (m, 1H), 3.94 (s, 3H), 3.93 (s, 3H), 3.63-3.55 (m, 2H), 3.22-3.10 (m, 2H), 2.45-2.41 (m, 2H), 2.33-2.29 (m, 2H), 2.22-1.93 (m, 4H), 1.76-1.73 (m, 2H), 1.66-1.59 (m, 2H), 1.46-1.41 (m, 4H). **^{13}C NMR** (100 MHz, CD_3OD) δ (ppm) = 174.6, 172.9, 161.0, 157.9, 152.8, 149.4, 137.9, 137.0, 133.5, 132.5, 131.3, 130.6, 130.4, 125.6, 122.3, 105.3, 104.3, 99.8, 57.3, 57.0, 49.5, 48.0, 37.8, 33.7, 29.9, 29.8, 26.7, 26.6. **HPLC purity**: 99%, RT 12.17 min. **LRMS (ESI):** *m*/*z* 657.3 $[M+H]^+$. **HRMS (ESI):** 656.3554 $[M+H]^+$, calculated for $[C_{36}H_{44}ClN_7O_5 + H^+]$ 656.3555 (Δ = 0.1 ppm).

N1-(4-((4-((1-(2-Fluorobenzyl)piperidin-4-yl)amino)-6,7-dimethoxyquinazolin-2-yl)amino)phenyl)-N8-hydroxyoctanediamide hydrochloride (**25b**)

Procedure G was following using: **24b** (154 mg, 0.20 mmol, 1.0 equiv.), 4M HCl/Dioxane (0.152 mL, 0.61 mmol, 3.0 equiv.) in 5 mL THF. The crude product was washed with DCM, further with DCM + 1 % MeOH to yield 15 mg (11%) of **25b** as pale white solid.

R_f = 0.20 (DCM/MeOH = 9:1 + 0.5% TEA). **^{1}H NMR** (400 MHz, CD_3OD) δ (ppm) = 7.72 (s, 1H), 7.86-7.66 (m, 8H), 7.04 (s, 1H), 4.40 (s, 2H), 4.37-4.34 (m, 1H), 3.96 (s, 3H), 3.95 (s, 3H), 3.60-3.56 (m, 2H), 3.19-3.06 (m, 2H), 2.44-2.41 (m, 2H), 2.34-2.29 (m, 2H), 2.10-2.07 (m, 3H), 1.76-1.61 (m, 5H), 1.45-1.38 (m, 4H). **^{13}C NMR** (100 MHz, CD_3OD) δ (ppm) = 173.3, 171.5, 160.5, 160.2, 159.7, 156.6, 151.6, 148.1, 136.8, 136.8, 135.7, 133.4, 132.6, 124.9, 124.5, 121.0, 115.8, 103.8, 102.9, 98.4, 55.8, 55.6, 51.4, 36.4, 32.3, 28.5, 28.4, 25.3, 25.1.

LRMS (ESI): *m/z* 675.30 $[M+H]^+$. **HRMS (ESI):** 674.3460 $[M+H]^+$, calculated for $[C_{36}H_{44}FN_7O_5 + H^+]$ 674.3461 (Δ = 0.2 ppm).

N1-(4-((4-((1-(2-Chlorobenzyl)piperidin-4-yl)amino)-6,7-dimethoxyquinazolin-2-yl)amino)phenyl)-N8-hydroxyoctanediamide 2,2,2-trifluoroacetate (**25c**)

Procedure G was following using **24c** (212 mg, 0.27 mmol, 1.0 equiv.), 4M HCl/Dioxane (0.20 mL, 0.82 mmol, 3 equiv.) in 5 mL THF. The crude product was washed with water, DCM, further purified using preparative HPLC resulting in the 10 mg (6%) of **25c** as a pale white solid.

R_f = 0.19 (DCM/MeOH = 9:1 + 0.5% TEA). **^{1}H NMR** (400 MHz, CD_3OD) δ (ppm) = 7.70-7.48 (m, 9H), 7.00 (s, 1H), 4.56 (s, 2H), 4.36-4.32 (m, 1H), 3.95 (s, 3H), 3.92 (s, 3H), 3.67-3.65 (m, 2H), 3.28-3.18 (m, 2H), 2.45-2.30 (m, 4H), 2.21-1.93 (m, 4H), 1.78-1.71 (m, 2H), 1.66-1.57 (m, 2H), 1.46-1.36 (m, 4H). **^{13}C NMR** (100 MHz, CD_3OD) δ (ppm) = 174.4, 161.1, 161.1, 158.0, 152.8, 149.4, 137.7, 137.2, 137.0, 134.8, 134.0, 133.3, 131.5, 129.1, 128.6, 125.3, 122.4, 105.1, 104.1, 99.7, 57.0, 57.0, 53.3, 49.3, 48.4, 37.8, 29.9, 29.8, 26.7, 26.5. **HPLC purity**: 93%, RT 10.87 min. **LRMS (ESI):** *m/z* 691.30 $[M+H]^+$. **HRMS (ESI):** 690.3176 $[M+H]^+$, calculated for $[C_{36}H_{44}ClN_7O_5 + H^+]$ 690.3165 (Δ = 1.6 ppm).

N1-(4-((6,7-Dimethoxy-4-((1-(4-methoxybenzyl)piperidin-4-yl)amino)quinazolin-2-yl)amino)phenyl)-N8-hydroxyoctanediamide hydrochloride (**25d**)

Procedure G was following using: **24d** (148 mg, 0.19 mmol, 1.0 equiv.), 4M HCl/Dioxane (0.145 mL, 0.58 mmol, 3.0 equiv.) in 5 mL THF. The crude product was washed with DCM, further purified in preparative HPLC using Acetonitrile: Water system to yield 40 mg (31%) of **25d** as a pale brown solid.

R_f = 0.16 (DCM/MeOH = 9:1 + 0.5% TEA). **^{1}H NMR** (400 MHz, CD_3OD) δ (ppm) = 7.63-7.42 (m, 7H), 7.03-7.01 (m, 2H), 6.90 (s, 1H), 4.30 (s, 2H), 4.26-4.20 (m, 1H), 3.92 (s,

3H), 3.84 (s, 3H), 3.82 (s, 3H), 3.55-3.52 (m, 2H), 3.14-3.05 (m, 2H), 2.43-2.39 (m, 2H), 2.30-2.26 (m, 3H), 2.11-2.08 (m, 3H), 1.76-1.70 (m, 2H), 1.64-1.59 (m, 2H), 1.46-1.35 (m, 4H). **^{13}C NMR** (100 MHz, CD_3OD) δ (ppm) = 175.9, 174.5, 172.9, 162.5, 160.8, 157.7, 152.6, 149.2, 137.4, 137.3, 133.9, 124.6, 122.5, 122.1, 115.6, 105.2, 104.1, 99.8, 61.0, 57.3, 56.9, 55.9, 51.2, 49.6, 37.8, 33.7, 30.0, 29.8, 26.7, 26.5. **HPLC purity**: 99%, RT 11.03 min. **LRMS (ESI):** *m/z* 687.30 $[M+H]^+$. **HRMS (ESI):** 686.3668 $[M+H]^+$, calculated for $[C_{37}H_{47}N_7O_6 + H^+]$ 686.3661 (Δ = 1.1 ppm).

N1-(4-((4-((1-(4-Fluorobenzyl)piperidin-4-yl)amino)-6,7-dimethoxyquinazolin-2-yl)amino)phenyl)-N8-hydroxyoctanediamide hydrochloride (**25e**)

Procedure G was following using: **24e** (193 mg, 0.25 mmol, 1.0 equiv.), 4M HCl/Dioxane (0.190 mL, 0.76 mmol, 3.0 equiv.) in 5 mL THF. The crude product was washed with DCM, further with DCM + 1 % MeOH to yield 17 mg (10%) of **25e** as a pale brown solid.

R_f = 0.17 (DCM/MeOH = 9:1 + 0.5% TEA). **^{1}H NMR** (400 MHz, CD_3OD) δ (ppm) = 7.64-7.61 (m, 5H), 7.45-7.43 (m, 2H), 7.24 (t, *J*= 8.9 Hz, 2H), 6.98 (s, 1H), 4.36 (s, 2H), 4.34-4.30 (m, 1H), 3.94 (s, 3H), 3.90 (s, 3H), 3.57-3.54 (m, 2H), 3.15-3.09 (m, 2H), 2.44-2.39 (m, 2H), 2.33-2.24, (m, 3H), 2.13-2.05 (m, 3H), 1.78-1.69 (m, 2H), 1.65-1.58 (m, 2H), 1.47-1.37 (m, 4H). **^{13}C NMR** (100 MHz, CD_3OD) δ (ppm) = 177.8, 174.7, 172.9, 161.0, 157.9, 153.0, 149.4, 137.9, 137.3, 134.7, 133.7, 131.5, 125.6, 122.3, 117.0, 105.2, 104.3, 99.9, 60.8, 57.2, 56.9, 52.6, 49.3, 37.8, 34.9, 33.7, 30.0, 29.4, 26.7. **HPLC purity**: 97%, RT 12.3 min. **LRMS (ESI):** *m/z* 675.3 $[M+H]^+$. **HRMS (ESI):** 674.3466 $[M+H]^+$, calculated for $[C_{36}H_{44}FN_7O_5 + H^+]$ 674.3461 (Δ = 0.7 ppm).

7-((4-((1-Benzylpiperidin-4-yl)amino)-6,7-dimethoxyquinazolin-2-yl)amino)-N-hydroxyheptanamide (**25f**)

Procedure G was following using: **24f** (20 mg, 0.032 mmol, 1.0 equiv.), 4M HCl/Dioxane (0.024 mL, 0.096 mmol, 3.0 equiv.) in 5 mL THF. The crude product was washed with DCM, further with DCM to yield 8 mg (47%) of **25f** as a brown solid.

R_f = 0.22 (DCM/MeOH = 9:1 + 0.5% TEA). **^{1}H NMR** (400 MHz, (CD_3OD) δ (ppm) = 7.69 (s, 1H), 7.60-7.52 (m, 6H), 4.55-4.50 (m, 1H), 4.42 (s, 2H), 3.97 (s, 3H), 3.93 (s, 3H), 3.66-3.62 (m, 2H), 3.53-3.44 (m, 2H), 3.29-3.19 (m, 2H), 2.44-2.35 (m, 2H), 2.14-2.06 (m, 4H), 1.72-1.64 (m, 4H), 1.51-1.38 (m, 4H). **^{13}C NMR** (100 MHz, CD_3OD) δ (ppm) = 172.8, 161.0, 154.1, 149.6, 149.1, 137.0, 132.6, 131.3, 130.4, 130.7, 105.5, 99.2, 61.7, 57.2, 56.9, 52.7, 49.5, 42.4, 29.6, 29.5, 27.6, 27.5, 26.5. **HPLC purity**: 84%, RT 10.83 min**. MS** (ESI) 537.20 $[M+H]^+$.

8-(4-(4-((1-Benzylpiperidin-4-yl)amino)-6,7-dimethoxyquinazolin-2-yl)piperazin-1-yl)-N-hydroxy-8-oxooctanamide hydrochloride (**25g**)

Procedure G was following using: **24g** (18 mg, 0.025 mmol, 1.0 equiv.), 4M HCl/Dioxane (0.018 mL, 0.075 mmol, 3.0 equiv.) in 5 mL THF. The crude residue was triturated with DCM and DCM/MeOH (99:1) to yield 14 mg (97%) of **25g** as a pale white solid.

R_f = 0.25 (DCM/MeOH = 9:1 + 0.004% NH_4OH). **^{1}H NMR** (400 MHz, CD_3OD), δ (ppm) = 7.74 (s, 1H), 7.63-7.58 (m, 3H), 7.53-7.49 (m, 2H), 7.22 (s, 1H), 4.69-4.58 (m, 1H), 4.38 (s, 2H), 4.03-4.00 (m, 2H), 3.97(s, 3H), 3.94 (s, 3H), 3.92-3.89 (m, 2H), 3.82-3.77 (m, 4H), 3.62-3.57 (m, 2H), 3.42-3.33 (m, 2H), 2.52-2.46 (m, 2H), 2.37-2.30 (m, 3H), 2.18-2.09 (m, 3H), 1.68-1.60 (m, 4H), 1.45-1.37 (m, 4H). **^{13}C NMR** (100 MHz, $CDCl_3$), δ (ppm) = 176.0, 174.6, 172.9, 160.2, 157.7, 152.9, 149.4, 137.2, 132.5, 131.3, 130.5, 105.2, 103.8, 99.9, 61.8, 57.3, 57.0, 52.7, 48.2, 46.0, 45.6, 42.0, 34.71, 33.9, 29.91, 29.5, 26.2, 25.9. **HPLC purity:** 99%, RT 10.82 min **MS** (ESI) 634.3 $[M+H]^+$.

N1-(4-((4-((1-Benzylpiperidin-4-yl)amino)thieno[3,2-d]pyrimidin-2-yl)amino)phenyl)-N8-hydroxyoctanediamide 2,2,2-trifluoroacetate (**25h**)

Procedure G was following using: **24h** (61 mg, 0.088 mmol, 1.0 equiv.), 4M HCl/Dioxane (0.070 mL, 0.266 mmol, 3.0 equiv.) in 5 mL THF. The crude hydroxamic acid product was washed with DCM, further purified in preparative HPLC using Acetonitrile: Water system to yield 1.6 mg (0.03%) of **25h** as a pale orange solid.

R_f = 0.19 (DCM/MeOH = 9:1 + 0.5% TEA). **^{1}H NMR** (400 MHz, CD_3OD), δ (ppm) = 8.15 (d, *J* = 5.7 Hz, 1H), 7.67-7.61 (m, 4H), 7.50 (m, 3H), 7.45-7.43 (m, 2H), 7.27 (d, *J* = 5.7 Hz, 1H), 4.40 (s, 2H), 4.36-4.30 (m, 1H), 3.61-3.53 (m, 2H), 3.24-3.13 (m, 2H), 2.45-2.42 (m, 2H), 2.31-2.26 (m, 2H), 2.11-1.99 (m, 3H), 1.80-1.70 (m, 2H), 1.66-1.58 (m, 2H), 1.47-1.29 (m, 5H). **^{13}C NMR** (100 MHz, CD_3OD), δ (ppm) = 174.7, 172.9, 158.7, 158.6, 154.0, 148.3, 138.2, 138.0, 133.5, 132.5, 131.3, 130.4, 125.9, 122.3, 118.7, 110.6, 61.6, 52.7, 49.7, 37.8, 34.8, 33.7, 29.8, 26.7, 26.6, 25.9. **HPLC purity**: 98%, RT 10.68 min**. MS** (ESI) 602.30 $[M+H]^+$.

Ligand Docking

The crystal structure of HDAC1 (PDB id 4BKX), HDAC2 (PDB id 5IWG), HDAC3 (PDB id 4A69) and HDAC6 (PDB id 5EDU) were downloaded from the PDB and used a started point to study **25d** interactions with HDACs. The chemical structure of **25d** were sketched, built and docked using the docking module of ICM-Pro software v 1.8-7b (www.molsoft.com). The charges were assigned using the internal coordinate force field. The structures of HDACs were aligned and the grid maps were generated based on the scaffold of the co-crystalized ligand in HDAC6, which encompassed the entire binding site. The grid of size 30x30x30 Å3 was large enough to allow enough room for the rotation and translation of ligand molecules. Docking was carried out using automated docking module in ICM-Pro software, employing the default parameters. The final docked conformation of the ligands was chosen based on strongest binding energy between the docked ligand and the HDAC structures. The docked complex for

each ligand was chosen as the starting structure for further analysis. The docked structures were visualized and structural figures made using the MolSoft viewer.

Enzyme Assays

Enzyme inhibition assays were carried out by Reaction Biology Corporation (RBC).

HDAC assays: Add 2X of HDAC enzyme into reaction plate except control wells (no enzyme), where buffer (50 mM Tris-HCl, pH 8.0, 137 mM NaCl, 2.7 mM KCl, and 1 mM $MgCl_2$) is added instead [**Error! Bookmark not defined.**]. Add inhibitors in 100% DMSO into the enzyme mixture via acoustic technology (Echo550; nanoliter range). Spin down and pre-incubate. Add 2X Substrate Mixture: Fluorogenic HDAC General Substrate: 50 µM, Arg-His-Lys-Lys(Ac); HDAC8 only substrate: 50 µM, Arg-His-Lys(Ac)-Lys(Ac); Class2A Substrate: Acetyl-Lys(trifluoroacetyl)-AMC) in all reaction wells to initiate the reaction. Spin and shake. Incubate for 2 h at 30°C with seal. Add developer with Trichostatin A to stop the reaction and to generate fluorescent color. Carry out kinetic measurement for 1.5 h with Envision with 15 min interval. (Ex/Em= 360/460 nm). Take endpoint reading for analysis after the development reaches plateau. IC_{50} values and curve fits were obtained using Prism (GraphPad Software).

Methyltransferase assay: Methyltransferase assays were performed in the radioisotope-based HotSpot format. The substrates were prepared in freshly prepared reaction buffer [**Error! Bookmark not defined.**]. The reaction buffer for EZH1 and EZH2 was 50mM Tris–HCl, pH 8.0, 50mM NaCl, 1mM EDTA, 1mM DTT, 1mM PMSF, and 1% DMSO. The reaction buffer for all other HMTs was 50mM Tris–HCl, pH 8.5, 50mM NaCl, 5mM MgCl2, 1mM DTT, 1mM PMSF, and 1% DMSO. Standard substrate concentrations were 5 mM peptide or protein substrate, and 1 mM SAM, unless otherwise mentioned. For control compound IC_{50} determinations, the test compounds were diluted in DMSO, and then added to the enzyme/substrate mixtures in nanoliter amounts by using an acoustic technology (Echo550;

Labcyte). The reaction was initiated by the addition of 3H-SAM, and incubated at 30_C for 1 h. The reaction was detected by a filter-binding method. Data analysis was performed using GraphPad Prism software for curve fits

Cellular assays

Cell lines KMS-12-BM, OPM-2, H929 (Multiple Myeloma Cell Lines) and MOLM-14 (Acute Myeloid Leukaemia Cell Line) were cultured in (RPMI)-1640 media (HyClone Laboratories Inc., Logan, Utah, USA) supplemented with 1% (v/v) Penicillin/Streptomycin (Biowest, Rue de la Caille, Nuaille, France), 1% (v/v) L-Glutamine (Sigma-Aldrich) and 10% (v/v) fetal bovine serum (FBS; Biowest) at 37°C in a humidified atmosphere with 5% CO2. Human breast cancer

Cell Viability Assays: Cells were plated in 96-well plates (Corning Inc., NY, USA) at 25,000 cells per well and then treated with indicated compounds at concentrations of up to 10µM for 48 h. All of the samples were done in triplicate and cell viability was monitored at the endpoint using CellTiter-Glo (CTG) Luminescent Cell Viability Assay (Promega, Madison, WI, USA) according to the manufacturer's instructions. The cytotoxicity induced by each treatment was calculated as the percentage of cell viability of each sample compared with the solvent-treated (control) cells. Dose-response curves were plotted to determine the half-maximal inhibitory concentration (IC_{50}) for each compound.

Immunoblotting: Cell lines were treated with indicated concentrations of compounds for 24 h. Cells were then harvested, washed twice with cold PBS and pelleted at 350 x g in 4°C for 5 minutes. Whole-cell extracts were then prepared by lysing the cell pellets in ice using cold RIPA lysis buffer (25 mM Tris-HCl pH 7.6, 150 mM NaCl, 1% NP-40, 1% sodium deoxycholate, 0.1% sodium dodecyl sulphate) supplemented with fresh protease and phosphatase inhibitor cocktails (Merck Millipore, Darmstadt, Germany). Lysates were

repeatedly vortexed for 30 minutes and centrifuged at 14,000 x g in 4°C for 20 minutes. Protein quantification was performed using BCA protein assay kit (Pierce, Rockford, IL, USA) according to manufacturer's instructions. Equal amounts of protein were loaded into each lane and resolved using 7.5–15% SDS-PAGE. Proteins were electrotransferred onto PVDF membranes (Millipore, Bedford, MA, USA), blocked with 5% non-fat milk for an hour at room temperature, and probed with indicated antibody overnight at 4°C. The blots were subsequently washed, incubated with HRP-conjugated secondary antibodies for an hour at room temperature, and detected by chemiluminescence (Amersham ECL,GE Healthcare, Buckinghamshire, UK). Antibodies against cleaved poly-adenosine di-phosphate ribose polymerase N214 (PARP; no. 9541S), acetylated histone 3 (no. 9677S), histone 3 (no. 9715S), dimethyl histone-3 lysine 9 (H3K9-Me2) (no.9753S) were purchased from Cell Signaling Technologies (Danvers, MA, USA). Antibody against α-tubulin (T9026) was from Sigma-Aldrich whereas antibodies against acetylated α-tubulin (no. sc-23950), GAPDH (no. sc-47724) as well as HRP-linked secondary antibodies (no. sc-2031, mouse; no. sc-2030, rabbit) were all obtained from Santa Cruz Biotechnology Inc. (Dallas, Texas, USA).

Cell lines MDA-MB-231 and MCF-7 (breast cancer cells) were purchased from ATCC (Rockville, MD). MDA-MB-231 and MCF-7 cells were grown in Dulbecco's Modified Eagle Medium (DMEM, Sigma Aldrich, Singapore), which was supplemented with 10% foetal bovine serum, 50 µg / mL penicillin and 50 µg/mL streptomycin at 37°C, 5% CO_2. The cells were sub-cultured to 80% confluency and used within 15-28 passages for the assay. Cell viability was assessed using MTT reagent (Sigma Aldrich) reconstituted with phosphate buffer saline (pH = 7.4).

Cell viability assays: MDA-MB-231, MCF-7 cells were seeded at 2500 cells per well in a 96-well plate for 24 h. The final concentrations of the test compounds were: 100 µM, 50 µM, 25 µM, 12.5 µM, 6.25 µM, 3.125 µM, 1.56 µM, 0.78 µM and 0.39 µM. Aliquots of the test

compounds (initially prepared as 100 mM stock solutions in DMSO and serially diluted) were added to each well and the plates were incubated for 72 h. The percentage of DMSO in all the wells was maintained at 0.1% v/v. At the end of incubation period, 200 µL per well of MTT solution (in DMEM) was added and the plates were incubated for another 3 h. After the formation of purple coloured formazan crystals, 100 µL DMSO was added to the wells. The absorbance of the wells was read on a microplate reader (Tecan Infinite M200) at 490 nm. Cell viability was determined from readings of treated wells compared to control wells (absence of test compound) with correction of background absorbance. The IC_{50} (concentration required to reduce cell viability to 50% of control/untreated cells) was determined in triplicates on separate occasions, using two different stock solutions. Percent viability readings for each test compound were plotted against log concentration on GraphPad Prism (version 5.0, GraphPad Software, San Diego, CA), with constraints set at ≥ 0 and $\leq 100\%$. A sigmoidal curve was generated from which the IC_{50} was obtained.

Determination of Apoptosis

The Annexin V-FITC Apoptosis Detection Kit (BD Biosciences, Franklin Lakes, NJ) was used. MDA-MB-231 were seeded (500,000 cells/well) per well in 6-well plates with DMEM media (high glucose, supplemented with 10% FBS). The plates were incubated at 37ºC for 24 h (5% CO_2) to allow the cells to attach. The cells were treated with the test compounds (prepared in same media) and the plates were incubated for 48 h at three concentrations: 0.5 IC_{50}, IC_{50} and 1.5 IC_{50} in triplicate. Final concentration of DMSO per well was 0.1% v/v. Staurosporine was used as the positive control. After the specified time, the supernatant in the well was collected, the cell pellet was trypsinized, and further combined with the supernatant and pelleted by centrifugation (150g, 5 min). The cell pellet was rinsed twice with cold 1X PBS and suspended in the proprietary binding buffer (1X) to give a concentration of 10^6 cells per mL. An aliquot (100 µL) of the suspension containing 10^6 cells was transferred to the FACS tube (5 mL) to

which was added Annexin V-FITC solution (5 µL) and propidium iodide (PI) solution (5 µL). The solution is gently vortexed, incubated in the dark for 15 min at room temperature (25ºC), 400 µL of binding buffer (1X) is added to this. The sample was analyzed immediately or no later than 1 h, in which case it should be kept in ice and protected from light. Analysis was carried out on a FCS500 flow cytometer (Beckman Coulter, CA) using the FlowJo Software 3. Controls comprised untreated cells, cells exposed to Annexin V-FITC only, and cells exposed to PI only.

Pharmacokinetic and Toxicity Analysis

Solubility: The kinetic solubility of the compounds was determined using multiscreen filter plates from Millipore. A saturated solution of the test compound was prepared in Universal Buffer pH 7.4 (1% DMSO, v/v), agitated for a fixed period of time, filtered and the concentration of the filtrate determined by UV spectroscopy to give an estimate of solubility.

Permeability (P_e): Effective Permeabilities (P_e) of the compounds were determined by the parallel artificial membrane permeation assay (PAMPA).[58] In this investigation, permeability was assessed at pH7.4 over 2 different permeation times, 6h and 16h. Determinations were carried out at ambient temperature, around 23°C.

5 µL of the 1% lecithin/dodecane was pipetted into the well of the donor plate. 300 µL of 50 µM compound solution was added to the well in the donor plate, and 300 µL of 1×PBS buffer was added into the corresponding well in the acceptor plate. After 6 h and 6 h, 250 µL/well of solution of donor wells and acceptor wells were transferred to separate wells in a 96-well UV plate. The absorbance of the solution was determined at 314 nm on a microplate reader.

In vitro metabolic stability in rat liver microsomes (RLM): Incubation mixtures consisted of 7.5 µL of 20 mg/mL FRLM and MRLM (final: 0.3 mg microsome protein/mL), 2.5 µL of 600 µM **25d** in acetonitrile (final: 3.0 µM), 440 µL of 0.1 M phosphate buffer (pH 7.4).[59] The

mixture was first shaken for 5 min for pre-incubation in a shaking water bath at 37ºC. Reaction was initiated by adding 50 µL of 10 mM NADPH to obtain a final concentration of 1mM NADPH in the mixture. The total volume of the reaction mixture was 500 µL. For metabolic stability studies, aliquots of 50 µL of the incubation sample mixture were collected at 0, 5, 10, 15, 30, and 45 min. After collection of samples, the reaction was terminated with 100 µL of chilled acetonitrile containing the internal standard. The mixture was then centrifuged at 10,000 X g to remove the protein and the supernatant was subsequently applied to LC-MS/MS analysis. Positive control (PC) samples were prepared as described above, except the test compound was replaced with the known P450 substrate (Midazolam, 3 µM). The samples were assayed for the degradation of midazolam to evaluate the adequacy of the experimental conditions for drug metabolism study. Negative control samples were also prepared as described above but without NADPH.

Toxicity assays on AC-10 and TAMH cells

AC-10 (Cardiomyocytes): Reference compound: Doxorubicin. AC-10 cells were seeded at a cell density of 5000 cells/well (75,000 cells/ml) in a 96-well plate (NUNC) for 24 h. Cells were then treated across a wide concentration range 100-0.315 µM. Drug-treated cells were then incubated at 37 °C for 24 hours. After 24 hours, cell viability was determined with CellTiter-Glo® Cell Viability Assay (Promega Corporation) as per manufacturer's instructions. The cell-reagent mixture was then transferred to a solid white flat-bottom 96-well plate (Greiner) for luminescence reading. Luminescence was then recorded with an integration time of 0.25 second with a Tecan Infinite® M200 Microplate reader. Either percentage inhibition at the top concentration or an IC_{50} was calculated as for the cell assays above. ***TAMH (Transforming growth factor-alpha mouse hepatocyte):*** Reference compound: Acetaminophen. TAMH cells were seeded at a cell density of 12,000 cells/well (60,000 cells /ml) in a 96 well plate (NUNC)

a day before treatment. The cells were then treated and analysed as discussed above for AC-10 cell toxicity assay.

AMES test for genotoxicity: *S. typhimurium* strains were grown from bacterial discs in nutrient broth at 37°C in a shaking incubator (~150 rpm) for about 10 h. The cultures were then measured for absorbance with a UV spectrophotometer at 660 nm. Cultures are ready for experiment at a density of approximately 1.0 to 1.2 absorbance reading

The top agar was melted in a hot water bath or microwave oven and 2 ml volumes were aliquot into culture tubes. The tubes of agar were then maintained at 45°C for at least 30 to 45 minutes for temperature equilibration. The controls (100 µl of DMSO and 2-AA) and the compounds were added to separate tubes containing top agar. To all the tubes containing either controls or drug compounds, 500 µl of S9 mix was added to the top agar.100 µl of *S. typhimurium strain* (either TA98 or TA100) was added to the top agar. The top agar containing all components from Steps 2-4 were immediately mixed and decant onto Minimal Glucose Agar Plate and swirled to obtain an even distribution of plating mixture over the agar surface. After agar was set to harden, the plates were then incubated in a 37°C incubator for 48 hours. Colonies were counted and recorded.

48-hour reinvasion assay for IC_{50} determination in *Plasmodium falciparum* (3D7 and K1 strains)

Ring-stage parasites were synchronized 1 cycle before the start of assay and resuspended to assay conditions of 1.25% hematocrit and 0.7% parasitemia (for 3D7) or 1% parasitemia (for K1). Reference antimalarial drugs and test compounds were then added to assay wells. After 48-hour incubation in the dark at 37°C, parasite labelling was carried out with 1µg/ml Hoechst 33342 (Molecular Probes) for 15 minutes at 37°C and at least 20,000 events were acquired with CyAn ADP Analyzer (Dako/Beckman Coulter, Brea, CA, USA). Fluorescence detection of Hoechst 33342, which stains parasite DNA, was carried out using excitation wavelength

405nm and emission wavelength 450±25nm. Results were analyzed using the FlowJo software, version 9.3.2. Values were obtained from at least 3 separate experiments.

ASSOCIATED CONTENT

Supporting Information. SI contains additional synthesis of compounds, ^{1}H and ^{13}CNMR spectra of all final compounds, HRMS and HPLC spectra for compounds **25a-e**, IC_{50} curves against HDACs, Methyltransferases, MDA-MB-231 and MCF-7, docking image against DNMT1. This material is available free of charge via the Internet at http://pubs.acs.org.

AUTHOR INFORMATION

Corresponding Author

* Email: bwdnus@gmail.com

Author Contributions

The manuscript was written through contributions of all authors. All authors have given approval to the final version of the manuscript.

Funding Sources

This research was funded by generous grants from the National University of Singapore (Drug Development Unit grant R-711-000-022-133 (PMR) and Faculty of Science start-up grant R-148-000-169-133 to BD). WJC is supported by NMRC Singapore Translation Research Investigator award and partly supported by a Singapore Cancer Syndicate Grant, the National Research Foundation Singapore and the Singapore Ministry of Education under the Research Centers of Excellence initiative. Research from the KSWT laboratory has been generously supported by a grant from the National Medical Research Council (NMRC/1310/2011).

ACKNOWLEDGMENTS

The authors gratefully acknowledge the NUS Drug Development Unit (http://ddu.nus.edu.sg/) for technical support, Ms Sheela David Packiaraj and Associate Professor Ho Han Kiat for providing toxicity data on TAMH, AC10, Ames, Dr Yang Shilli and Professor Paul Ho for RLM data and Mr. Yong Jun and Associate Professor Go Mei Lin for PK data.

ABBREVIATIONS

CQ: Chloroquine

DCM: Dicholoromethane

DIPEA: *N*,*N*-Diisopropylethylamine

DNMT: DNA Methyltransferase

HATU: Hexafluorophosphate Azabenzotriazole Tetramethyl Uronium

HDAC: Histone Deacetylase

MLM: Mouse Liver Microsome

MT: Methyltransferase

PARP: Poly ADP ribose polymerase

PI: Propidium iodide

PK: Pharmacokinetics

PS: Phosphotidylserine

PTM: Post-translational modifications

RLM: Rat Liver Microsome

SAHA: Suberanilohydroxamic Acid

THP: Tetrahydropyranol

References:

[1] Ke, X.; Shen, L. Molecular Targeted Therapy of Cancer: The Progress and Future Prospect. *Front. Lab. Med.* **2017**, *1* (2), 69–75.

[2] Aggarwal, S. Targeted Cancer Therapies. *Nat. Rev. Drug Discov.* **2010**, *9*, 427–428.

[3] Heerboth, S.; Lapinska, K.; Snyder, N.; Leary, M.; Rollinson, S.; Sarkar, S. Use of Epigenetic Drugs in Disease: An Overview. Genet. *Epigenetics* **2014**, *1* (6), 9–19.

[4] Malmquist, N. A.; Moss, T. A.; Mecheri, S.; Scherf, A.; Fuchter, M. J. Small-Molecule Histone Methyltransferase Inhibitors Display Rapid Antimalarial Activity against All Blood Stage Forms in Plasmodium Falciparum. *Proc. Natl. Acad. Sci.* **2012**, *109* (41), 16708–16713.

[5] Falkenberg, K. J.; Johnstone, R. W. Histone Deacetylases and Their Inhibitors in Cancer, Neurological Diseases and Immune Disorders. *Nat. Rev. Drug Discov.* **2014**, *13* (9), 673–691.

[6] Nicholson, T. B.; Veland, N.; Chen, T. *An Introduction to Epigenetic Mediators in Cancer*; 2015.

[7] Huang, J.; Dorsey, J.; Chuikov, S.; Zhang, X.; Jenuwein, T.; Reinberg, D.; Berger, S. L. G9a and Glp Methylate Lysine 373 in the Tumor Suppressor P53. *J. Biol. Chem.* **2010**, *285* (13), 9636–9641.

[8] Ren, A.; Qiu, Y.; Cui, H.; Fu, G. Inhibition of H3K9 Methyltransferase G9a Induces Autophagy and Apoptosis in Oral Squamous Cell Carcinoma. *Biochem. Biophys. Res. Commun.* **2015**, *459* (1), 10–17.

[9] Vedadi, M.; Barsyte-Lovejoy, D.; Liu, F.; Rival-Gervier, S.; Allali-Hassani, A.; Labrie, V.; Wigle, T. J.; Dimaggio, P. A.; Wasney, G. A.; Siarheyeva, A.; Dong, A.; Tempel, W.; Wang, S. C.; Chen, X.; Chau, I.; Mangano, T. J.; Huang, X. P.; Simpson, C. D.; Pattenden, S. G.; Norris, J. L.; Kireev, D. B.; Tripathy, A.; Edwards, A.; Roth, B. L.; Janzen, W. P.; Garcia, B. A.; Petronis, A.; Ellis, J.; Brown, P. J.; Frye, S. V.; Arrowsmith, C. H.; Jin, J. A Chemical Probe Selectively Inhibits G9a and GLP Methyltransferase Activity in Cells. *Nat. Chem. Biol.* **2011**, *7* (8), 566–574.

[10] Liu, F.; Barsyte-lovejoy, D.; Li, F.; Xiong, Y.; Korboukh, V. K.; Huang, X.; Allali-hassani, A.; Janzen, W. P.; Roth, B. L.; Frye, V.; Arrowsmith, C. H.; Brown, P. J.; Vedadi, M.; Jin, J. Discovery of an in Vivo Chemical Probe of the Lysine Methyltransferases G9a and GLP. *J. Med. Chem.* **2013**, *56* (21), 8931–8942.

[11] Pappano, W. N.; Guo, J.; He, Y.; Ferguson, D.; Jagadeeswaran, S.; Osterling, D. J.; Gao, W.; Spence, J. K.; Pliushchev, M.; Sweis, R. F.; Buchanan, F. G.; Michaelides, M. R.; Shoemaker, A. R.; Tse, C.; Chiang, G. G. The Histone Methyltransferase Inhibitor A-366 Uncovers a Role for G9a/GLP in the Epigenetics of Leukemia. *PLoS One* **2015**, *10* (7), 1–13.

[12] Curry, E.; Green, I.; Chapman-Rothe, N.; Shamsaei, E.; Kandil, S.; Cherblanc, F. L.; Payne, L.; Bell, E.; Ganesh, T.; Srimongkolpithak, N.; Caron, J.; Li, F.; Uren, A. G.; Snyder, J. P.; Vedadi, M.; Fuchter, M. J.; Brown, R. Dual EZH2 and EHMT2 Histone Methyltransferase Inhibition Increases Biological Efficacy in Breast Cancer Cells. *Clin. Epigenetics* **2015**, *7* (1), 1–12.

[13] Haberland, M.; Montgomery, R. L.; Olson, E. N. The Many Roles of Histone Deacetylases in Development and Physiology: Implications for Disease and Therapy. *Nat. Rev. Genet.* **2009**, *10* (1), 32–42.

[14] Dokmanovic, M.; Clarke, C.; Marks, P. A. Histone Deacetylase Inhibitors: Overview and Perspectives. *Mol. Cancer Res.* **2007**, *5* (10), 981–989.

[15] Sumanadasa, S. D. M.; Goodman, C. D.; Lucke, A. J.; Skinner-Adams, T.; Saham, I.; Haque, A.; Do, T. A.; McFadden, G. I.; Fairlie, D. P.; Andrews, K. T. Antimalarial Activity of the Anticancer Histone Deacetylase Inhibitor SB939. *Antimicrob. Agents Chemother.* **2012**, *56* (7), 3849–3856.

[16] Wu, L.-P.; Wang, X.; Li, L.; Zhao, Y.; Lu, S.; Yu, Y.; Zhou, W.; Liu, X.; Yang, J.; Zheng, Z.; Zhang, H.; Feng, J.; Yang, Y.; Wang, H.; Zhu, W.-G. Histone Deacetylase Inhibitor Depsipeptide Activates Silenced Genes through Decreasing Both CpG and H3K9 Methylation on the Promoter. *Mol. Cell. Biol.* **2008**, *28* (10), 3219–3235.

[17] Fang, S.; Miao, J.; Xiang, L.; Ponugoti, B.; Treuter, E.; Kemper, J. K. Coordinated Recruitment of Histone Methyltransferase G9a and Other Chromatin-Modifying Enzymes in SHP-Mediated Regulation of Hepatic Bile Acid Metabolism. *Mol. Cell. Biol.* **2007**, *27* (4), 1407–1424.

[18] Cao, Z.; Hong, R.; Ding, B.; Zuo, X.; Li, H.; Ding, J.; Li, Y.; Huang, W.; Zhang, Y. TSA and BIX-01294 Induced Normal DNA and Histone Methylation and Increased Protein Expression in Porcine Somatic Cell Nuclear Transfer Embryos. *PLoS One* **2017**, *12* (1), 1–15.

[19] Zimmermann, G. R.; Leh??r, J.; Keith, C. T. Multi-Target Therapeutics: When the Whole Is Greater than the Sum of the Parts. *Drug Discov. Today* **2007**, *12* (1–2), 34–42.

[20] José-Enériz, E. S.; Agirre, X.; Rabal, O.; Vilas-Zornoza, A.; Sanchez-Arias, J. A.; Miranda, E.; Ugarte, A.; Roa, S.; Paiva, B.; De Mendoza, A. E. H.; María Alvarez, R.; Casares, N.; Segura, V.; Martín-Subero, J. I.; Ogi, F. X.; Soule, P.; Santiveri, C. M.; Campos-Olivas, R.; Castellano, G.; De Barrena, M. G. F.; Rodriguez-Madoz, J. R.; García-Barchino, M. J.; Lasarte, J. J.; Avila, M. A.; Martinez-Climent, J. A.; Oyarzabal, J.; Prosper, F. Discovery of First-in-

Class Reversible Dual Small Molecule Inhibitors against G9a and DNMTs in Hematological Malignancies. *Nat. Commun.* **2017**, *8* (May).

[21] Patra, S. K.; Patra, A.; Dahiya, R. Histone Deacetylase and DNA Methyltransferase in Human Prostate Cancer. *Biochem. Biophys. Res. Commun.* **2001**, *287* (3), 705–713.

[22] Chu-Farseeva, Y. yi; Mustafa, N.; Poulsen, A.; Tan, E. C.; Yen, J. J. Y.; Chng, W. J.; Dymock, B. W. Design and Synthesis of Potent Dual Inhibitors of JAK2 and HDAC Based on Fusing the Pharmacophores of XL019 and Vorinostat. *Eur. J. Med. Chem.* **2018**, *158*, 593–619.

[23] Yao, L.; Mustafa, N.; Tan, E. C.; Poulsen, A.; Singh, P.; Duong-Thi, M. D.; Lee, J. X. T.; Ramanujulu, P. M.; Chng, W. J.; Yen, J. J. Y.; Ohlson, S.; Dymock, B. W. Design and Synthesis of Ligand Efficient Dual Inhibitors of Janus Kinase (JAK) and Histone Deacetylase (HDAC) Based on Ruxolitinib and Vorinostat. *J. Med. Chem.* **2017**, *60* (20), 8336–8357.

[24] Yang, E. G.; Mustafa, N.; Tan, E. C.; Poulsen, A.; Ramanujulu, P. M.; Chng, W. J.; Yen, J. J. Y.; Dymock, B. W. Design and Synthesis of Janus Kinase 2 (JAK2) and Histone Deacetlyase (HDAC) Bispecific Inhibitors Based on Pacritinib and Evidence of Dual Pathway Inhibition in Hematological Cell Lines. *J. Med. Chem.* **2016**, *59* (18), 8233–8262.

[25] Guerrant, W.; Patil, V.; Canzoneri, J. C.; Yao, L.; Hood, R.; Oyelere, A. K. Bioorganic & Medicinal Chemistry Letters Dual-Acting Histone Deacetylase-Topoisomerase I Inhibitors. **2013**, *23*, 3283–3287.

[26] Bhatia, S.; Krieger, V.; Groll, M.; Osko, J.; Reßing, N.; Ahlert, H.; Borkhardt, A.; Kurz, T.; Christianson, D. W.; Hauer, J.; Hansen, F. K. Discovery of the First-in-Class Dual Histone Deacetylase-Proteasome Inhibitor. *J. Med. Chem.* **2018**, acs.jmedchem.8b01487.

[27] Falahi, F.; van Kruchten, M.; Martinet, N.; Hospers, G. A. P.; Rots, M. G. Current and Upcoming Approaches to Exploit the Reversibility of Epigenetic Mutations in Breast Cancer. *Breast Cancer Res.* **2014**, *16* (4), 412.

[28] Zang, L.; Kondengaden, S. M.; Zhang, Q.; Li, X.; Sigalapalli, D. K.; Kondengadan, S. M.; Huang, K.; Li, K. K.; Li, S.; Xiao, Z.; Wen, L.; Zhu, H.; Babu, B. N.; Wang, L.; Che, F.; Wang, P. G. Structure Based Design, Synthesis and Activity Studies of Small Hybrid Molecules as HDAC and G9a Dual Inhibitors. *Oncotarget* **2017**, *8* (38), 63187–63207.

[29] Mahendran, A.; Ngo, L.; Venta-perez, G.; Megan, L.; Breslow, R.; Marks, P. A.; Lee, J.; Yao, Y.; Mahendran, A.; Ngo, L.; Venta-perez, G.; Choy, M. L. Correction for Lee et Al., Development of a Histone Deacetylase 6 Inhibitor and Its Biological Effects. *Proc. Natl. Acad. Sci.* **2015**, *112* (43), E5899–E5899.

[30] Abagyan, R.; Totrov, M.; Kuznetsov, D. New Method for Protein Modeling and Design: Applications to Docking and Structure Prediction From. **1994**, *15* (5), 488–506.

[31] Matthias, J. MRT - Mono Boc Protection of Diamines. *Aldrich ChemFiles* **2009**, *9.4*, 12.

[32] Xu, C.; Soragni, E.; Chou, C. J.; Herman, D.; Plasterer, H. L.; Rusche, J. R.; Gottesfeld, J. M. Chemical Probes Identify a Role for Histone Deacetylase 3 in Friedreich's Ataxia Gene Silencing. *Chem. Biol.* **2009**, *16* (9), 980–989.

[33] Applewhite, T. H.; Nelson, J. S. Preparation of Amides. 3,264,281, 1966.

[34] Rho, H.; Baek, H.; Kim, D.; Chang, I. A Convenient Method for the Preparation of Alkanolamides. *Bull. Korean Chem. Soc.* **2006**, *27* (4), 584–586.

[35] Chan, L. C.; Cox, B. G.; Couplings, N.-H. H.; Pr, A.; Road, S.; Park, I.; Way, C. Kinetics of Amide Formation through Carbodiimide / N- Hydroxybenzotriazole (HOBt) Couplings Kinetics of Amide Formation through Carbodiimide /. *J. Org. Chem.* **2007**, No. 3, 8863–8869.

[36] Liu, F.; Chen, X.; Allali-Hassani, A.; Quinn, A. M.; Wasney, G. a; Dong, A.; Barsyte, D.; Kozieradzki, I.; Senisterra, G.; Chau, I.; Siarheyeva, A.; Kireev, D. B.; Jadhav, A.; Herold, J. M.; Frye, S. V; Arrowsmith, C. H.; Brown, P. J.; Simeonov, A.; Vedadi, M.; Jin, J. Discovery of a 2,4-Diamino-7-Aminoalkoxyquinazoline as a Potent and Selective Inhibitor of Histone Lysine Methyltransferase G9a. *J. Med. Chem.* **200 Cyanohydridoborate anion as a selective reducing agent 9**, *52* (24), 7950–7953.

[37] Borch, R. F.; Bernstein, M. D.; Durst, H. D. Cyanohydridoborate anion as a selective reducing agent *J. Am. Chem. Soc.* **1971**, *93*, 2897–2904

[38] Nudelman, A.; Bechor, Y.; Falb, E.; Fischer, B.; Wexler, B. a.; Nudelman, A. Acetyl Chloride-Methanol as a Convenient Reagent for: A) Quantitative Formation of Amine Hydrochlorides B) Carboxylate Ester Formation C) Mild Removal of N-t-Boc-Protective Group. *Synth. Commun.* **1998**, *28*, 471–474.

[39] Giannini, G.; Marzi, M.; Pezzi, R.; Brunetti, T.; Battistuzzi, G.; Marzo, M. Di; Cabri, W.; Vesci, L.; Pisano, C. N-Hydroxy-(4-Oxime)-Cinnamide: A Versatile Scaffold for the Synthesis of Novel Histone Deacetilase (HDAC) Inhibitors. *Bioorg. Med. Chem. Lett.* **2009**, *19* (8), 2346–2349.

[40] Lobera, M.; Madauss, K. P.; Pohlhaus, D. T.; Wright, Q. G.; Trocha, M.; Schmidt, D. R.; Baloglu, E.; Trump, R. P.; Head, M. S.; Hofmann, G. A.; Murray-Thompson, M.; Schwartz, B.; Chakravorty, S.; Wu, Z.; Mander, P. K.; Kruidenier, L.; Reid, R. A.; Burkhart, W.; Turunen, B. J.; Rong, J. X.; Wagner, C.; Moyer, M. B.; Wells, C.; Hong, X.; Moore, J. T.; Williams, J. D.; Soler, D.; Ghosh, S.; Nolan, M. A. Selective Class IIa Histone Deacetylase Inhibition via a Nonchelating Zinc-Binding Group. *Nat. Chem. Biol.* **2013**, *9* (5), 319–325.

[41] De Vreese, R.; Van Steen, N.; Verhaeghe, T.; Desmet, T.; Bougarne, N.; De Bosscher, K.; Benoy, V.; Haeck, W.; Van Den Bosch, L.; D'Hooghe, M. Synthesis of Benzothiophene-Based Hydroxamic Acids as Potent and Selective HDAC6 Inhibitors. *Chem. Commun.* **2015**, *51* (48), 9868–9871.

[42] Leonhardt, M.; Sellmer, A.; Krämer, O. H.; Dove, S.; Elz, S.; Kraus, B.; Beyer, M.; Mahboobi, S. Design and Biological Evaluation of Tetrahydro-β-Carboline Derivatives as

Highly Potent Histone Deacetylase 6 (HDAC6) Inhibitors. *Eur. J. Med. Chem.* **2018**, *152*, 329–357.

[43] De Vreese, R.; Galle, L.; Depetter, Y.; Franceus, J.; Desmet, T.; Van Hecke, K.; Benoy, V.; Van Den Bosch, L.; D'hooghe, M. Synthesis of Potent and Selective HDAC6 Inhibitors Bearing a Cyclohexane- or Cycloheptane-Annulated 1,5-Benzothiazepine Scaffold. *Chem. - A Eur. J.* **2017**, *23* (1), 128–136.

[44] Hsieh, H. Y.; Chuang, H. C.; Shen, F. H.; Detroja, K.; Hsin, L. W.; Chen, C. S. Targeting Breast Cancer Stem Cells by Novel HDAC3-Selective Inhibitors. *Eur. J. Med. Chem.* **2017**, *140*, 42–51.

[45] Trivedi, P.; Adhikari, N.; Amin, S. A.; Jha, T.; Ghosh, B. Design, Synthesis and Biological Screening of 2-Aminobenzamides as Selective HDAC3 Inhibitors with Promising Anticancer Effects. *Eur. J. Pharm. Sci.* **2018**, *124* (August), 165–181.

[46] Li, X.; Inks, E. S.; Li, X.; Hou, J.; Chou, C. J.; Zhang, J.; Jiang, Y.; Zhang, Y.; Xu, W. Discovery of the First N -Hydroxycinnamamide-Based Histone Deacetylase 1/3 Dual Inhibitors with Potent Oral Antitumor Activity. *J. Med. Chem.* **2014**, *57* (8), 3324–3341.

[47] Bresciani, A.; Ontoria, J. M.; Biancofiore, I.; Cellucci, A.; Ciammaichella, A.; Di Marco, A.; Ferrigno, F.; Francone, A.; Malancona, S.; Monteagudo, E.; Nizi, E.; Pace, P.; Ponzi, S.; Rossetti, I.; Veneziano, M.; Summa, V.; Harper, S. Improved Selective Class I and Novel Selective HDAC3 Inhibitors: Beyond Hydroxamic Acids and Benzamides. *ACS Med. Chem. Lett.* **2018**, acsmedchemlett.8b00517.

[48] Horiuchi, K. Y.; Eason, M. M.; Ferry, J. J.; Planck, J. L.; Walsh, C. P.; Smith, R. F.; Howitz, K. T.; Ma, H. Assay Development for Histone Methyltransferases. *Assay Drug Dev. Technol.* **2013**, *11* (4), 227–236.

[49] Rotili, D.; Tarantino, D.; Marrocco, B.; Gros, C.; Masson, V.; Poughon, V.; Ausseil, F.; Chang, Y.; Labella, D.; Cosconati, S.; Di Maro, S.; Novellino, E.; Schnekenburger, M.; Grandjenette, C.; Bouvy, C.; Diederich, M.; Cheng, X.; Arimondo, P. B.; Mai, A. Properly Substituted Analogues of BIX-01294 Lose Inhibition of G9a Histone Methyltransferase and Gain Selective Anti-DNA Methyltransferase 3A Activity. *PLoS One* **2014**, *9* (5), 1–9.

[50] Lee, J. Y. C.; Kuo, C. W.; Tsai, S. L.; Cheng, S. M.; Chen, S. H.; Chan, H. H.; Lin, C. H.; Lin, K. Y.; Li, C. F.; Kanwar, J. R.; Leung, E. Y.; Cheung, C. C. H.; Huang, W. J.; Wang, Y. C.; Cheung, C. H. A. Inhibition of HDAC3- and HDAC6-Promoted Survivin Expression Plays an Important Role in SAHA-Induced Autophagy and Viability Reduction in Breast Cancer Cells. *Front. Pharmacol.* **2016**, *7* (MAR), 1–13.

[51] Huang, L.; Pardee, a B. Suberoylanilide Hydroxamic Acid as a Potential Therapeutic Agent for Human Breast Cancer Treatment. *Mol. Med.* **2000**, *6* (10), 849–866.

[52] Chun, P. Histone Deacetylase Inhibitors in Hematological Malignancies and Solid Tumors. *Arch. Pharm. Res.* **2015**, *38* (6), 933–949.

[53] Cheng, F.; Xia, B.; Sahakian, E.; Lwin, T.; Wang, H.; Xing, L.; Shah, B. D.; PerezVillarroel, P.; LienlafMoreno, M.; Zhang, Y.; Quayle, S. N.; Jones, S. S.; Pinilla-Ibarz, J.; Villagra, A.; Sotomayor, E. M.; Tao, J. Selective Inhibition of Histone Deacetylase 6 (HDAC6) and HDAC3 As a Novel Therapeutic Strategy in Mantle Cell Lymphoma (MCL). *Blood* **2014**, *124* (21), 5397–5397.

[54] Richardson, P. G.; Elghandour, A.; Jedrzejczak, W. W.; Guenther, A.; Nakorn, T. N.; Siritanaratkul, N.; Schlossman, R. L.; Hou, J.; Moreau, P.; Lonial, S.; Lee, J. H.; Einsele, H.; Sopala, M.; Bengoudifa, B.; Corrado, C.; Binlich, F. Panobinostat plus Bortezomib and Dexamethasone in Previously Treated Multiple Myeloma : Outcomes by Prior Treatment. **2018**, *127* (6), 713–722.

[55] Kubicek, S.; Sullivan, R. J. O.; August, E. M.; Hickey, E. R.; Zhang, Q.; Teodoro, M. L.; Rea, S.; Mechtler, K.; Kowalski, J. A.; Homon, C. A.; Kelly, T. A.; Jenuwein, T. Technique Reversal of H3K9me2 by a Small-Molecule Inhibitor for the G9a Histone Methyltransferase. *Mol. Cell* **2007**, *1*, 473–481.

[56] Sundriyal, S.; Malmquist, N. A.; Caron, J.; Blundell, S.; Liu, F.; Chen, X.; Srimongkolpithak, N.; Jin, J.; Charman, S. A.; Scherf, A.; Fuchter, M. J. Development of Diaminoquinazoline Histone Lysine Methyltransferase Inhibitors as Potent Blood-Stage Antimalarial Compounds. *ChemMedChem* **2014**, *9* (10), 2360–2373.

[57] Gilson, P. R.; Tan, C.; Jarman, K. E.; Lowes, K. N.; Curtis, J. M.; Nguyen, W.; Di Rago, A. E.; Bullen, H. E.; Prinz, B.; Duffy, S.; Baell, J. B.; Hutton, C. A.; Jousset Subroux, H.; Crabb, B. S.; Avery, V. M.; Cowman, A. F.; Sleebs, B. E. Optimization of 2-Anilino 4-Amino Substituted Quinazolines into Potent Antimalarial Agents with Oral in Vivo Activity. *J. Med. Chem.* **2017**, *60* (3), 1171–1188.

[58] Kerns, E. H.; Petusky, S.; Farris, M.; Ley, R.; Jupp, P. Combined Application of Parallel Artificial Membrane Permeability Assay and Caco-2 Permeability Assays in Drug Discovery. *J. Pharm. Sci.* **2004**, *93* (6), 1440–1453.

[59] Lu C, Li P, Gallegos R, Uttamsingh V, Xia C Q, Miwa G T, et al. Comparison of intrinsic clearance in liver microsomes and hepatocytes from rats and humans: evaluation of free fraction and uptake in hepatocytes. *Drug Metab. Dispos.* **2006**, *34* (9), 1600-1605.